L-Aspartate Links for Stable Sodium Metal-Organic Frameworks

Peter Siman, [†] Christopher A. Trickett, [†] Hiroyasu Furukawa[†‡] and Omar M. Yaghi*[†‡]

[†] Department of Chemistry, University of California - Berkeley, Materials Sciences Division, Lawrence Berkeley National Laboratory, and Kavli Energy NanoSciences Institute at Berkeley, Berkeley, California 94720, United States.

[‡] King Fahd University of Petroleum and Minerals, Dhahran 34464, Saudi Arabia.

Table of Content

1. Synthesis of organic linkers

1.1. General

All reactions were carried out under nitrogen unless otherwise noted. Dichloromethane (CH_2Cl_2), *N*,*N*-dimethylformamide (DMF), methanol, and diisopropelethylamine (DIPEA) were obtained from EMD Millipore Chemicals. Sodium hydroxide was purchased from Sigma-Aldrich. *N*,*N*-diethylformamide (DEF) was obtained from BASF SE. Other solvents and reagents were obtained from commercial sources and used without further purification.

Analytical techniques. Single crystal data were collected on a Bruker D8 Venture diffractometer using monochromatic fine focus Cu Kα radiation (λ = 1.54178 Å) operated at 50 kW and 1.0 mA and APEX II detector or on beamline 11.3.1 at the Advanced Light Source, Lawrence Berkeley National Lab. Samples were mounted on MiTeGen® kapton loops and placed in a 100(2) K nitrogen cold stream provided by an Oxford Cryostream 700 Plus low temperature apparatus on the goniometer head of a Bruker D8 diffractometer equipped with a PHOTON100 CMOS detector operating in shutterless mode. Scanning electron microscopy (SEM) images were taken on a Hitachi S-4800 scanning electron microscope operating at an accelerating voltage of 5 kV. Powder X-ray data were collected using a Bruker D8 Advance employing Ni filtered Cu Kα (λ = 1.54178 Å). The system was also outfitted with an anti-scattering shield that prevents incident diffuse radiation from hitting the detector. Samples were placed on zero background sample holders by dropping wet sample from a pipette and partially dried, or as powders from a spatula then leveled. The 2θ range was 2.5-50° with a step size of 0.02° and a fixed counting time of 1 s/step for dry samples and 0.16 s/step for wet samples. Thermogravimetric analysis (TGA) curves were recorded on a TA Q500 thermal analysis system under nitrogen flow. Elemental microanalyses (EA) were performed in the Microanalytical Laboratory of the College of Chemistry at UC Berkeley, using a Perkin Elmer 2400 Series II CHNS elemental analyzer. FTIR spectra were collected in-house using a Bruker ALPHA Platinum ATR-FTIR Spectrometer equipped with a single reflection diamond ATR module. Low-pressure N_2 and CO_2 adsorption isotherms were recorded on a Quantachrome Autosorb-1 volumetric gas adsorption analyzer. A liquid nitrogen bath was used for the N_2 measurements at 77 K, while the temperature was controlled with a water circulator for the 273 and 298 K CO_2 and N_2 isotherm measurements. Helium was used for the estimation of dead space for gas

adsorption measurements. Ultra-high-purity grade N_2, CO_2, and He gases (99.999% purity) were used throughout the experiments. ^1H and ^{13}C NMR spectra were acquired on a Bruker ARX-500 (500 MHz), DRX-500 (500 MHz), or AVB-400 (400 MHz) spectrometer at 297–300 K, and the chemical shifts were calculated using the solvent resonances as internal standards (^1H: 7.26 ppm for $CHCl_3$, 2.50 ppm for DMSO, 4.79 ppm for H_2O; $^{13}C\{^1H\}$: 77.00 ppm for $CDCl_3$, 39.51 ppm for DMSO-d_6. Analytical HPLC was performed on a Thermo instrument (Dionex Ultimate 3000) using an analytical column (Jupiter 5 micron, C18 300 Å 150 × 4.6 mm) at a flow rate of 1.2 mL/min and wavelength of 230 nm, where buffer A is 0.1% trifluoroacetic acid (TFA) in deionized water and buffer B is 0.1% TFA in acetonitrile. Electrospray Ionization (ESI) mass spectrometry was acquired using a Shimadzu LCMS-2020 instrument, using positive mode through direct injection. High Resolution Electrospray Ionization mass spectrometry (HR-ESI) was acquired on an Finnigan LTQ FT (Thermo Electron Corporation) instrument, using positive and negative modes and by direct injection of methanol solutions of the samples using a syringe pump with a flow rate of 5 μL min^{-1}. Column chromatography was performed on silica gel purchased from Sorbent Technologies (standard grade, 60 Å, 40–63 μm). Analytical thin layer chromatography (TLC) was performed on Whatman 250 μm-thick silica gel 60 plates with a fluorescent indicator. Visualization of TLC spots was accomplished with UV light at 254 nm and by staining with phosphomolybdic acid in ethanol.

1.2. Synthesis of (2S,2'S)-2,2'-(terephthaloylbis(azanediyl))disuccinic acid (H_4BDA) (1)

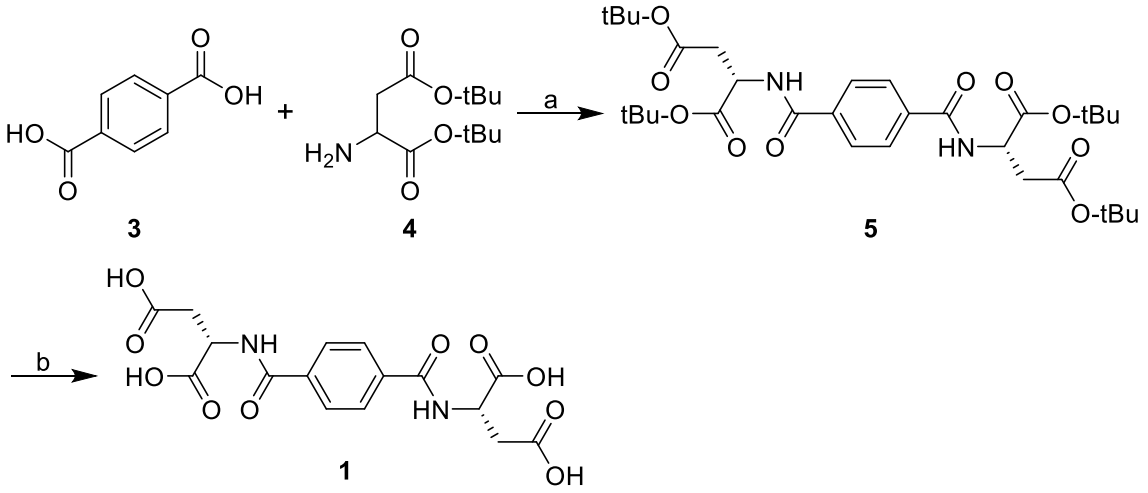

Scheme S1. (2*S*,2'*S*)-2,2'-(terephthaloylbis(azanediyl))disuccinic acid (H_4BDA).

a) DIC, HOBt, DIPEA in DCM, 0 °C-rt, 12 h, 70%; b) TFA in DCM (1:1), 0 °C-rt, 3 h, quntitative yield.

Synthesis of tetra-*tert*-butyl-2,2'-(terephthaloylbis(azanediyl))(2*S*,2'*S*)-disuccinate (**5**)

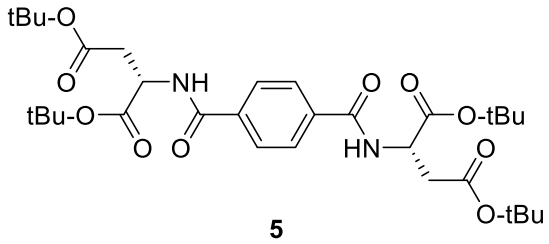

5

To a 100 mL round bottom flask equipped with a dropping funnel and magnetic stir bar, 0.70 g of terephthalic acid and 1.25 g of hydroxybenzotriazole (HOBt) were added along with 14 mL of dry DCM. In a separate vial, 2.1 g of L-aspartic acid di-*tert*-butyl ester hydrochloride was dissolved in 14 mL DCM followed by 1.6 mL of DIPEA (to deprotonate the amine and catalyze the reaction) then transferred to the dropping funnel. To the terephthalic acid solution, 1.5 mL of N,N'-diisopropylcarbodiimide (DIC) followed by 1.6 mL of DIPEA were added (the addition of DIPEA was the start point for the terephthalate activation). After 4-5 min from the addition of DIC, (the solution should become clear, if not DMF may be added until it is fully clear) the aspartic acid solution was added dropwise over 15 min.

After the reaction finished as indicated by TLC, 100 mL of EtOAc were added and the organic layer was extracted using saturated sodium bicarbonate solution ($NaHCO_3$, 3×40 mL) followed by 40 mL brine. The solution was then dried over $MgSO_4$, filtered and evaporated. The crude product was purified using flash chromatography to yield 1.8 g (70%) of pure white solid. R_f = 0.25 (ethyl acetate/*n*-hexane = 3/7). ^{1}H NMR (400 MHz, $CDCl_3$) δ 7.89 (s, 17H), 7.30 (s, 2H), 7.29 (s, 1H), 4.89 (dt, *J* = 8.1, 4.2 Hz, 3H), 3.08 – 2.83 (m, 5H), 1.51 (s, 21H), 1.47 (s, 21H). ^{13}C NMR (101 MHz, $CDCl_3$) δ 170.5, 169.8, 166.0, 136.9, 127.4, 82.7, 81.8, 77.1, 49.6, 37.4, 28.1, 27.9. ESI-MS: Calculated for $C_{32}H_{48}N_2O_{10}$: 620.7400 Da, Observed: 621.3373 Da [M+H^+], 643.3180 [M+Na^+].

Synthesis of (2*S*,2'*S*)-2,2'-(terephthaloylbis(azanediyl))disuccinic acid (H_4BDA) (**1**)

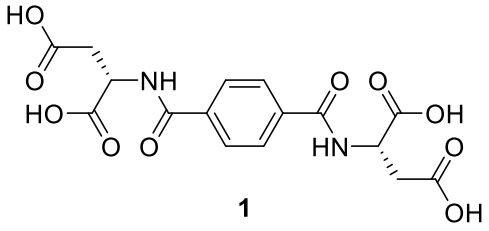

1

To the round bottom flask with the starting material (**5**), 9 mL DCM followed by 450 µL of triisopropylsilane (TIPS) were added, then the mixture was cooled in an ice bath. In a dropping funnel, 9 mL DCM and 18 mL TFA were mixed and added drop-wise to the cooled starting material. After the addition was finished, the reaction was allowed to stir at room temperature for another 3 h until all the starting material was consumed based on TLC. The solvent was dried, diluted with $CHCl_3$ and further dried. This process was repeated 3 times to remove traces of TFA and TIPS which yielded 1.00 g (96%) of white solid. R_f = 0.00 (ethyl acetate/n-hexane 3/7). ^{1}H NMR (500 MHz, D_2O) δ 7.68 (s, 1H), 4.84 (dd, *J* = 7.4, 5.2 Hz, 1H), 3.01 – 2.84 (m, 1H). ^{13}C NMR (126 MHz, D_2O) δ 174.30, 173.82, 169.67, 136.15, 127.59, 49.63, 35.32. ESI-MS: Calculated for $C_{16}H_{16}N_2O_{10}$: 396.3080 Da, Observed: 395.0728 Da [M-H^+].

1.3. Synthesis of (2*S*,2'*S*)-2,2'-(([1,1'-biphenyl]-4,4'-dicarbonyl)bis(azanediyl))disuccinic acid (H_4BPDA) (2)

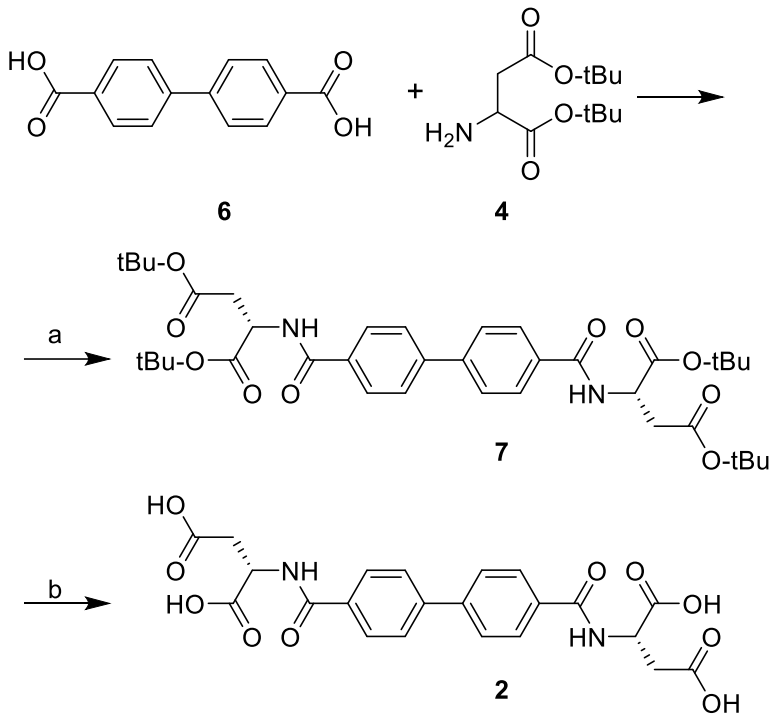

Scheme S2. (2*S*,2'*S*)-2,2'-(([1,1'-biphenyl]-4,4'-dicarbonyl)bis(azanediyl))disuccinic acid (H_4BPDA).

a) DIC, HOBt, DIPEA in DCM, 0 °C-rt, 12 h, 79%; b) TFA in DCM (1:1), 0 °C-rt, 3 h, quntitative yield.

Synthesis of tetra-*tert*-butyl 2,2'-(([1,1'-biphenyl]-4,4'-dicarbonyl)bis(azanediyl))(2*S*,2'*S*)-disuccinate (**7**)

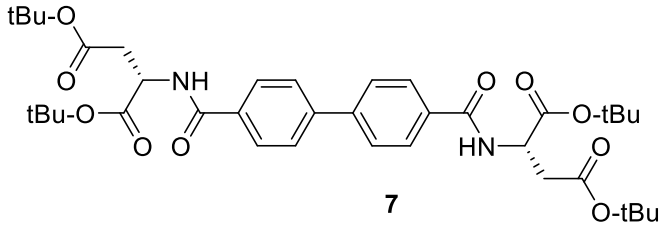

To a 100 mL round bottom flask equipped with a dropping funnel and magnetic stir bar, 1.02 g of [1,1'-biphenyl]-4,4'-dicarboxylic acid (H_2BPDC) (**5**) and 1.25 g of HOBt were added along with 28 mL dry DCM. In a separate vial, 2.1 g L-aspartic acid di-*tert*-butyl ester hydrochloride

was dissolved in 14 mL DCM, followed by 1.6 mL DIPEA (to deprotonate the amine and catalyze the reaction) then transferred to dropping funnel. To the H_2BPDC solution, 1.5 mL DIC followed by 1.6 mL DIPEA were added (the addition of DIPEA, was the start point for the terephthalate activation). After, 4-5 min from the addition of DIC (the solution should become clear, if not DMF may be added until it is fully clear), the aspartic acid solution was added drop wise through 15 min.

After the reaction finished as indicated by TLC, 100 mL EtOAc were added and the organic layer was extracted using saturated sodium bicarbonate ($NaHCO_3$, 3×40 mL) solution followed by 40 mL brine. This was then dried over $MgSO_4$ and evaporated. The crude was purified using flash chromatography to yield 2.2 g (79%) of pure white solid. R_f =0.25 (ethyl acetate/*n*-hexane = 3/7). ^{1}H NMR (500 MHz, $CDCl_3$) δ 7.92 (d, *J* = 8.5 Hz, 1H), 7.70 (d, *J* = 8.5 Hz, 1H), 7.31 (d, *J* = 7.9 Hz, 1H), 4.92 (dt, *J* = 8.2, 4.3 Hz, 1H), 2.96 (ddd, *J* = 60.4, 17.1, 4.3 Hz, 1H), 1.51 (s, 5H), 1.47 (s, 5H). ^{13}C NMR (126 MHz, $CDCl_3$) δ 170.55, 169.98, 166.44, 143.25, 133.37, 127.76, 127.38, 82.55, 81.67, 49.57, 37.52, 28.08, 27.94. ESI-MS: Calculated for $C_{38}H_{52}N_2O_{10}$: 696.8380 Da, Observed: 697.3686 Da [M+H^+], 719.3483 Da [M+Na^+].

Synthesis of (2S,2'S)-2,2'-(([1,1'-biphenyl]-4,4'-dicarbonyl)bis(azanediyl))disuccinic acid (H_4BPDA) (**2**)

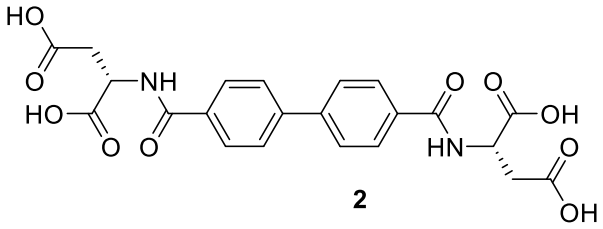

2

To the round bottom flask with the starting material (**7**), 18 mL DCM followed by 900 µL TIPS were added, then the mixture was cooled in an ice bath. In a dropping funnel 18 mL DCM and 36 mL TFA were mixed and added drop wise to the cooled starting material flask. After the addition was finished, the reaction was allowed to stir at room temperature for another 3 h until all the starting was consumed based on TLC. After reaction completion the solvent was dried, diluted with $CHCl_3$, and further dried. This process was repeated three times to remove traces of TFA which yielded 1.40 g (94%) of white solid. R_f = 0.00 (ethyl acetate/n-hexane 3/7). ^{1}H NMR

(500 MHz, DMSO-*d6*) δ 8.85 (d, J = 7.9 Hz, 1H), 7.98 (d, J = 8.5 Hz, 2H), 7.88 (d, J = 8.5 Hz, 2H), 4.78 (td, J = 8.0, 5.8 Hz, 1H), 2.92 – 2.67 (m, 2H). ^{13}C NMR (126 MHz, DMSO-*d6*) δ 173.05, 172.31, 166.12, 142.31, 133.59, 128.58, 127.25, 49.90, 36.24. ESI-MS: Calculated for $C_{22}H_{20}N_2O_{10}$: 472.4060 Da, Observed: 471.1037 Da [M-H$^+$].

Linkers **1** and **2** were used without any further purification.

2. Synthesis of single crystal MOFs

2.1 MOF-705

The synthesis of single crystal MOF was achieved by dissolving the H_4BDA (**1**) in DEF at 0.1 M. To a 4 mL scintillated vial, 2.5 mL of a freshly prepared solution of 10% (v/v) 1.0 M $NaOH_{(aq.)}$ in methanol were added. To the methanolic solution, 50 µL of the linker solution was added followed by swirling to homogenize the solution. This was followed by the addition of 50 µL of 1.0 M $Mg(NO_3)_2{\cdot}6H_2O$ solution in DEF.[1] The mixture was shaken briefly, tightly sealed[2] and placed in a 50 °C oven until needle shaped crystals precipitated at the bottom and on the walls (as-synthesized) with the dimensions of 0.01 × 0.01 × 0.05 mm^3. EA of the supercritical CO_2 (SC-CO_2) activated sample: Calcd. for $Na_8C_{34}H_{34}N_4O_{24}$ = Na_8(linker)$_2$(methanol)$_2$(H_2O)$_2$: C, 38.27; H, 3.19; N, 5.25. Found: C, 38.12; H, 2.66; N, 5.45%.

2.2 MOF-706

The same procedure described above was used, but instead with H_4BPDA **(2)** and with heating at 70 °C. The crystals dimensions were 0.05 × 0.05 × 0.03 mm^3. EA of the SC-CO_2 activated sample: Calcd. for $Na_8C_{34}H_{34}N_4O_{24}$ = Na_8(linker)$_2$(H_2O)$_4$: C, 36.68; H, 3.53; N, 5.52. Found: C, 36.78; H, 3.59; N, 3.82%.

2.3 Synthesis of Microcrystalline MOFs

The synthesis of microcrystalline MOFs with the average dimensions of 1 × 1 × 20 µm^3 was achieved by heating the reaction mixtures described above to 85 °C for 6-12 h.

2.4 MOFs activation

2.4.1 MOF-705

The resulting crystals were washed with methanol three times a day for four days. To remove the solvent from the MOF before final activation, it was treated using SC-CO_2 instrument which resulted in air stable crystals with a PXRD pattern matching the as-synthesized MOF. Full activation to remove the methanol and non-structural water molecules was achieved by evacuating the sample for 6 h at room temperature (RT) followed by heating to 70 °C for 6 h before cooling again to RT and finally purging with argon.

2.4.2 MOF-706

The resulting crystals were washed with methanol three times a day for 2 days, then with acetone four times a day for 2 days. To remove the solvent from the MOF, it was treated using SC-CO_2 followed by vacuum at RT for 6 h.

4. Analytical characterization

4.1 Digestion of MOF

4.1.1 NMR

MOF sample (ca. 2 mg) was placed in 0.6 mL DMSO-*d6* followed by 50 µL of 20% DCl, then sonicated for ~10 min (see NMR Figures S34 and S35).

4.1.2 LCMS

MOF sample (ca. 2 mg) was placed in 1.00 mL 25% acetonitrile in DIW with 0.1% TFA then sonicated for ~10 min in order to fully digest the MOF. Then 200 µL of sample was taken and subjected to RP-HPLC and compared to the R_t of pure linker as well as the mass. The results were the same as the pure linker (see Figures S36 and S37).

4.2 Single Crystal X-ray Diffraction Analyses

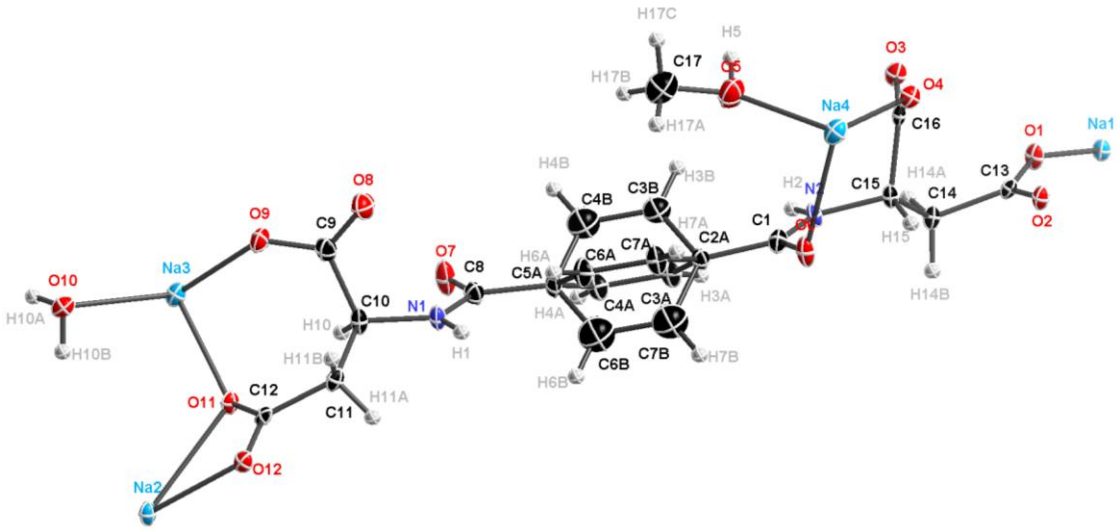

Figure S1. Asymmetric unit of MOF-705_as-synthesized.

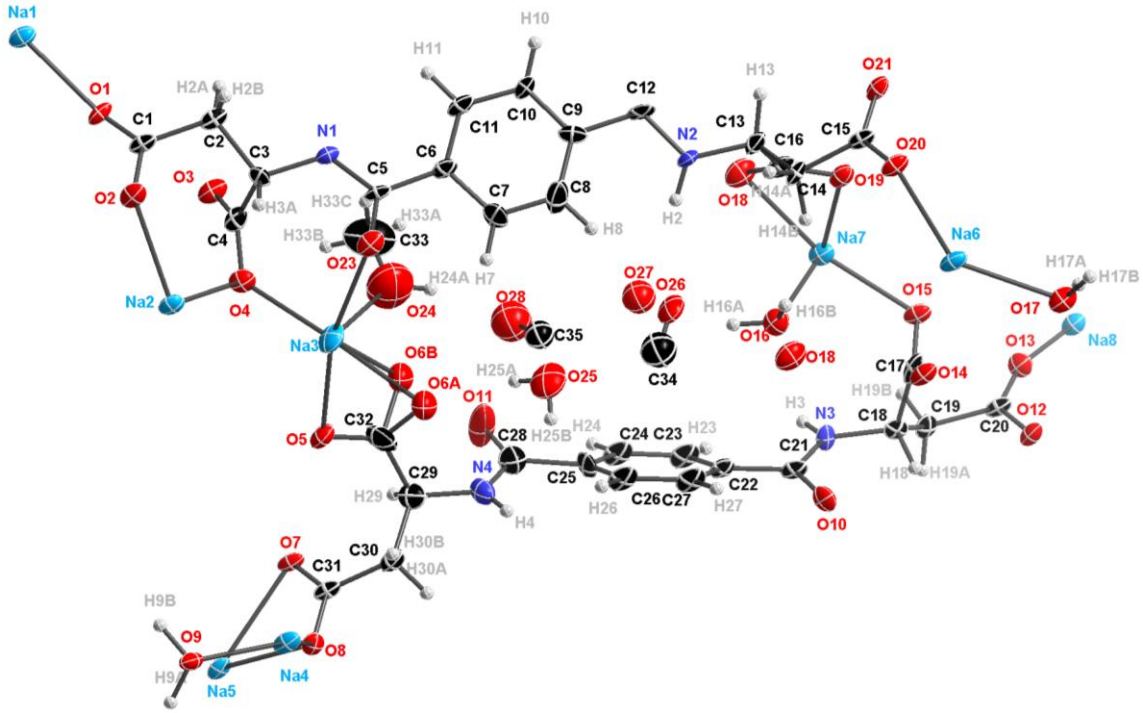

Figure S2. Asymmetric unit of MOF-705_sc.

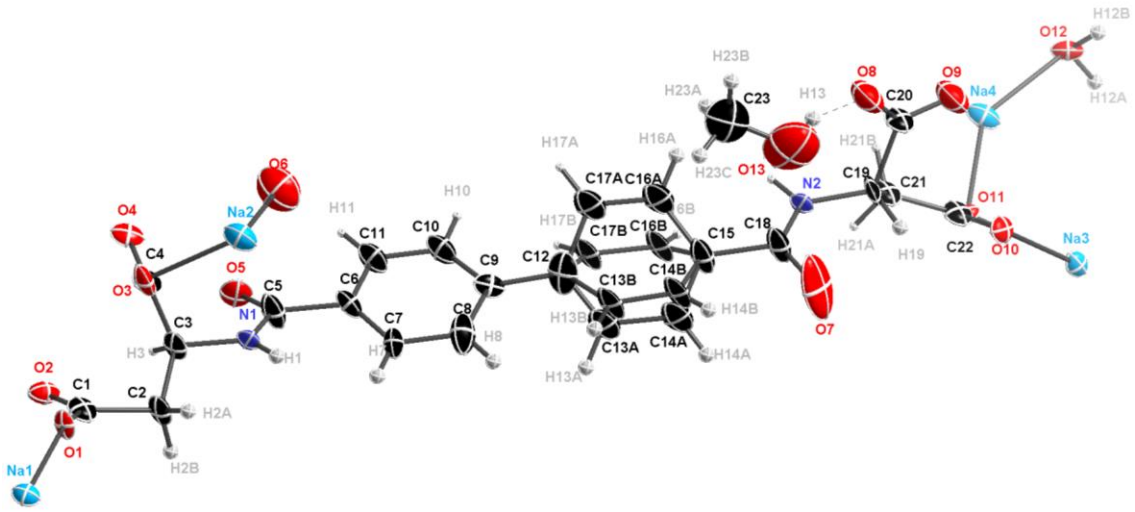

Figure S3. Asymmetric unit of MOF-706_as.

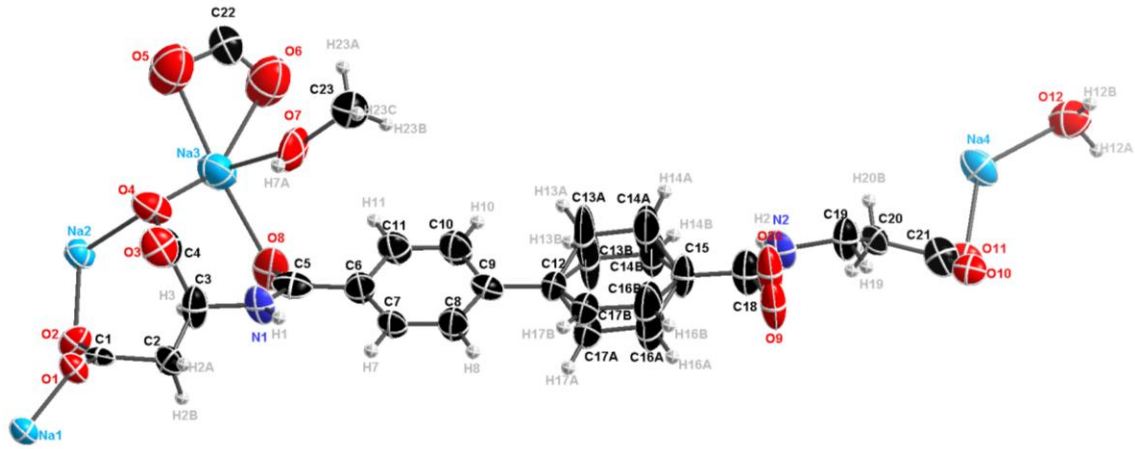

Figure S4. Asymmetric unit of MOF-706_sc.

Table S1. Crystallographic data of MOF-705 and MOF-706 in both stages, the as-synthesized (MOF-705_as and MOF-706_as) and the SC-CO_2 activated (MOF-705_sc and MOF-706_sc).

Sample	MOF-705_as	MOF-705_sc	MOF-706_as	MOF-706_sc
Chemical Formula	$C_{17}H_{18}N_2Na_4O_{12}$	$C_{33.08}H_{33.70}N_4Na_8O_{25.71}$	$C_{22.5}H_{18}N_2Na_4O_{12}$	$C_{22.25}H_{19.25}N_2Na_4O_{11.5}$
Formula mass	534.29	1082.58	618.87	590.61
Crystal system	monoclinic	monoclinic	monoclinic	monoclinic
Space group	$P2_1$	$P2_1$	$P2_1$	$P2_1$
λ [Å]	1.54178	0.77490	0.88560	1.03330
a [Å]	11.8894(4)	24.0448(19)[a]	12.0790(15)	11.9807(16)
b [Å]	5.2299(2)	5.2432(5)	5.2419(6)	5.2345(6)
c [Å]	17.4663(5)	16.9833(14)	21.254(3)	21.796(3)
β (degrees)	97.279(2)	103.366(6)	103.886(6)	99.274(10)
Z	2	2	2	2
V [Å^3]	1077.3(1)	2083.1(3)	1306.4(3)	1349.1(3)
T [K]	100(2)	100(2)	100(2)	100(2)
density [g cm^{-3}]	1.647	1.726	1.573	1.454
measured reflections	23262	18857	7646	6359
unique reflections	4415	4815	1594	1980
parameters	334	623	327	345
restraints	34	19	106	130
R_{int}	0.0889	0.1078	0.1134	0.1002
θ range (degrees)	2.55 - 74.52	2.568 - 23.539	2.164 - 21.724	2.504 - 28.238
R_1, wR_2	0.0415, 0.0965	0.0684, 0.1878	0.0721, 0.2093	0.1176, 0.3174
S (GOF)	1.037	1.009	1.007	1.273
max / min res. dens. [e Å^{-3}]	0.366 / -0.241	0.692 / -0.346	0.535 / -0.457	0.732 / -0.673

[a] the unit cell is doubled due to superstructure in which water and methanol coordinate to $Na_{(4)}$ alternatively.

4.3 Scanning Electron Microscope Images

Images of SC-CO_2 activated MOF-705 and MOF-706 were taken by dispersing each sample onto a sticky carbon surface attached to a flat aluminum sample holder.

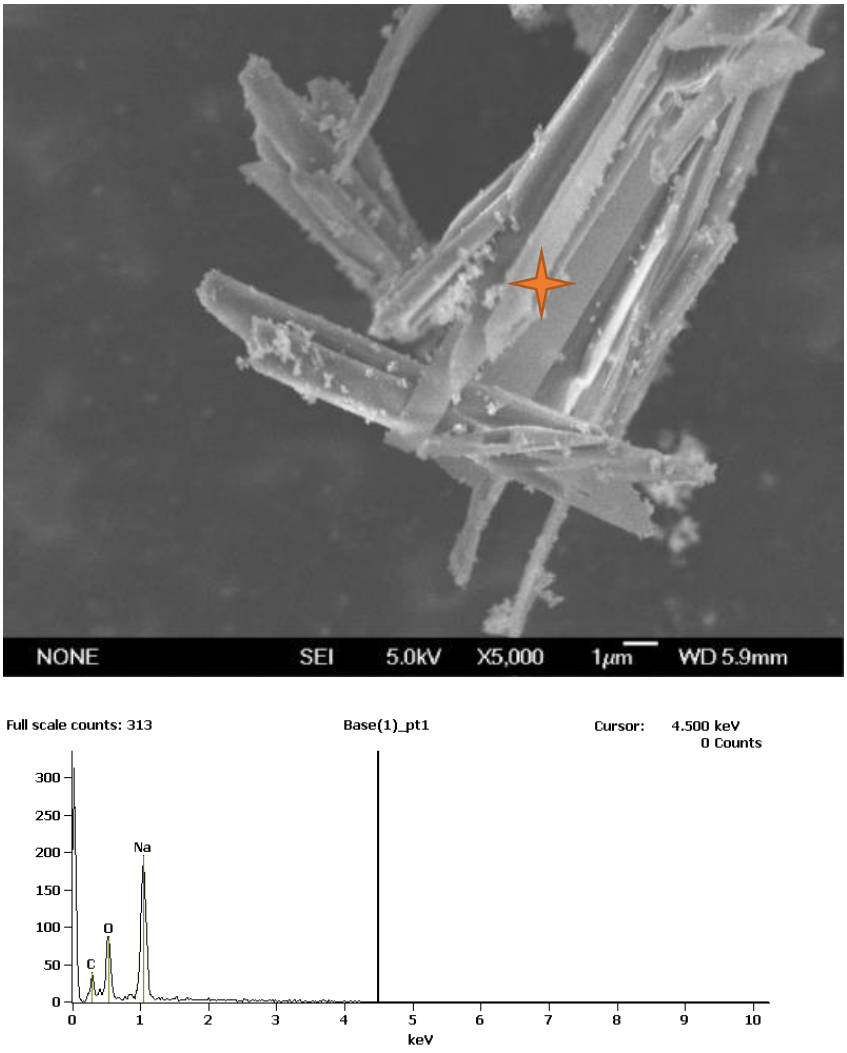

Figure S5. Scanning electron microscopy (SEM, top) image reveals the single-phase homogeneous morphology MOF-705. (Bottom) the orange star is example of energy dispersive spectroscopy (EDS) measurement taken to show the content of the material.

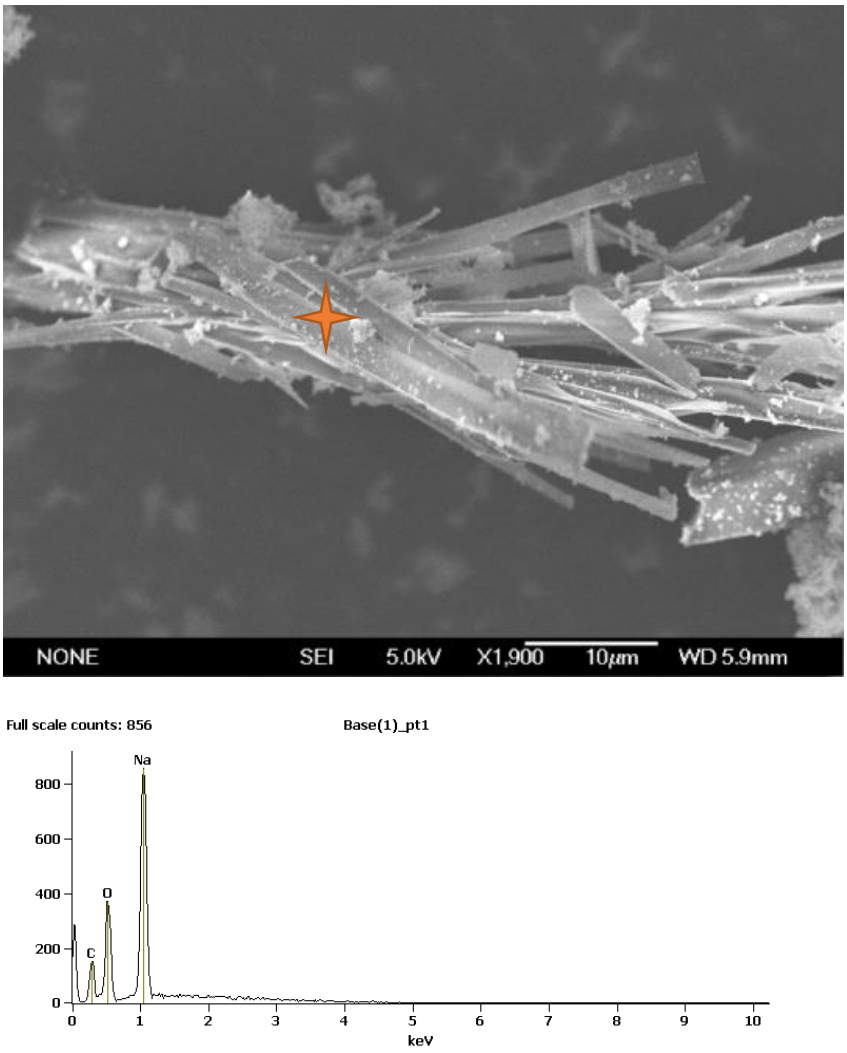

Figure S6. SEM image (top) reveals the single-phase homogeneous morphology of MOF-706. (Bottom) the orange star is example of EDS measurement taken to show the content of the material.

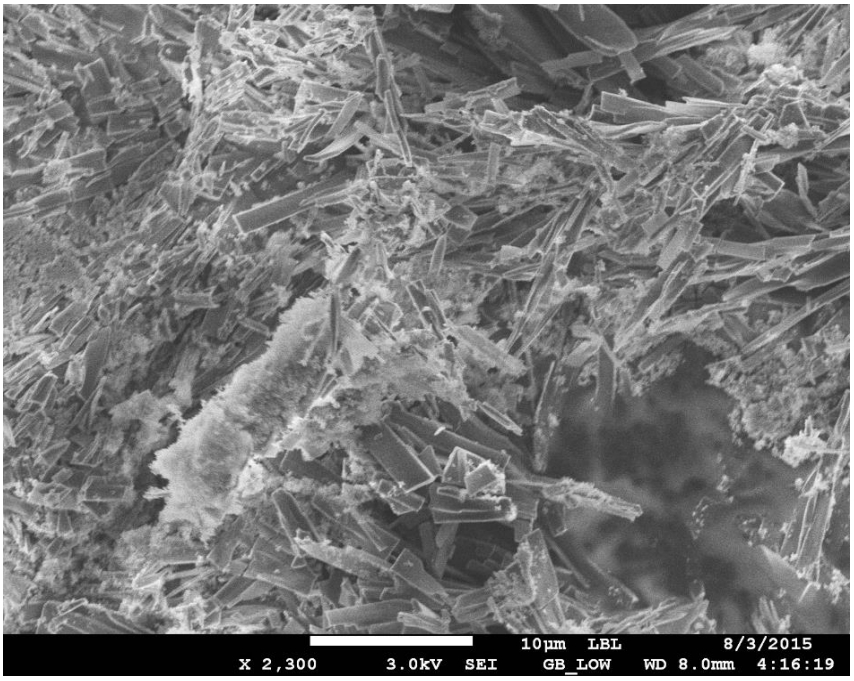

Figure S7. SEM image shows that MOF-705 is still crystalline after a month at ambient conditions.

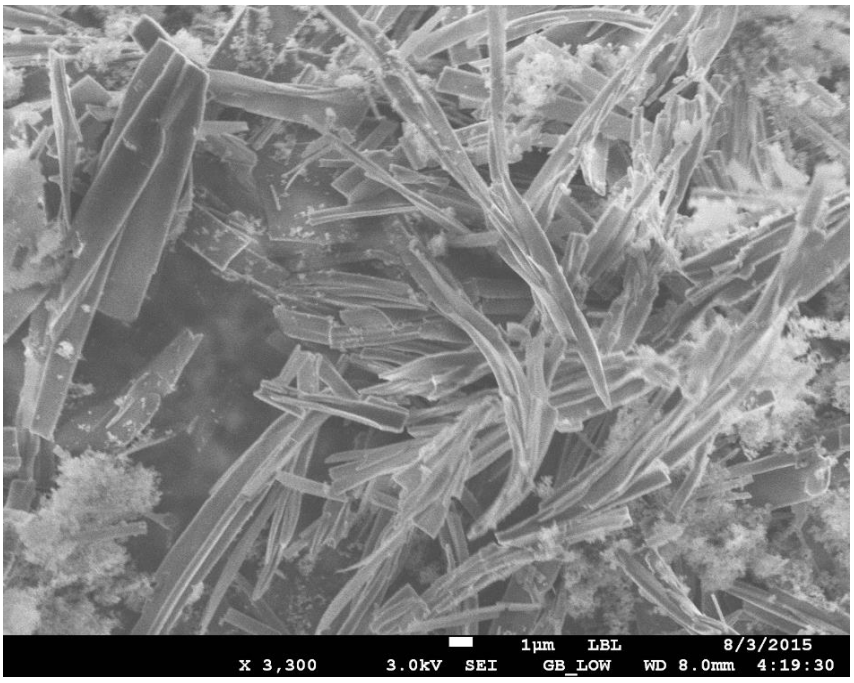

Figure S8. SEM image shows that MOF-706 is still crystalline after a month at ambient conditions.

4.4 Powder X-ray Diffraction Patterns

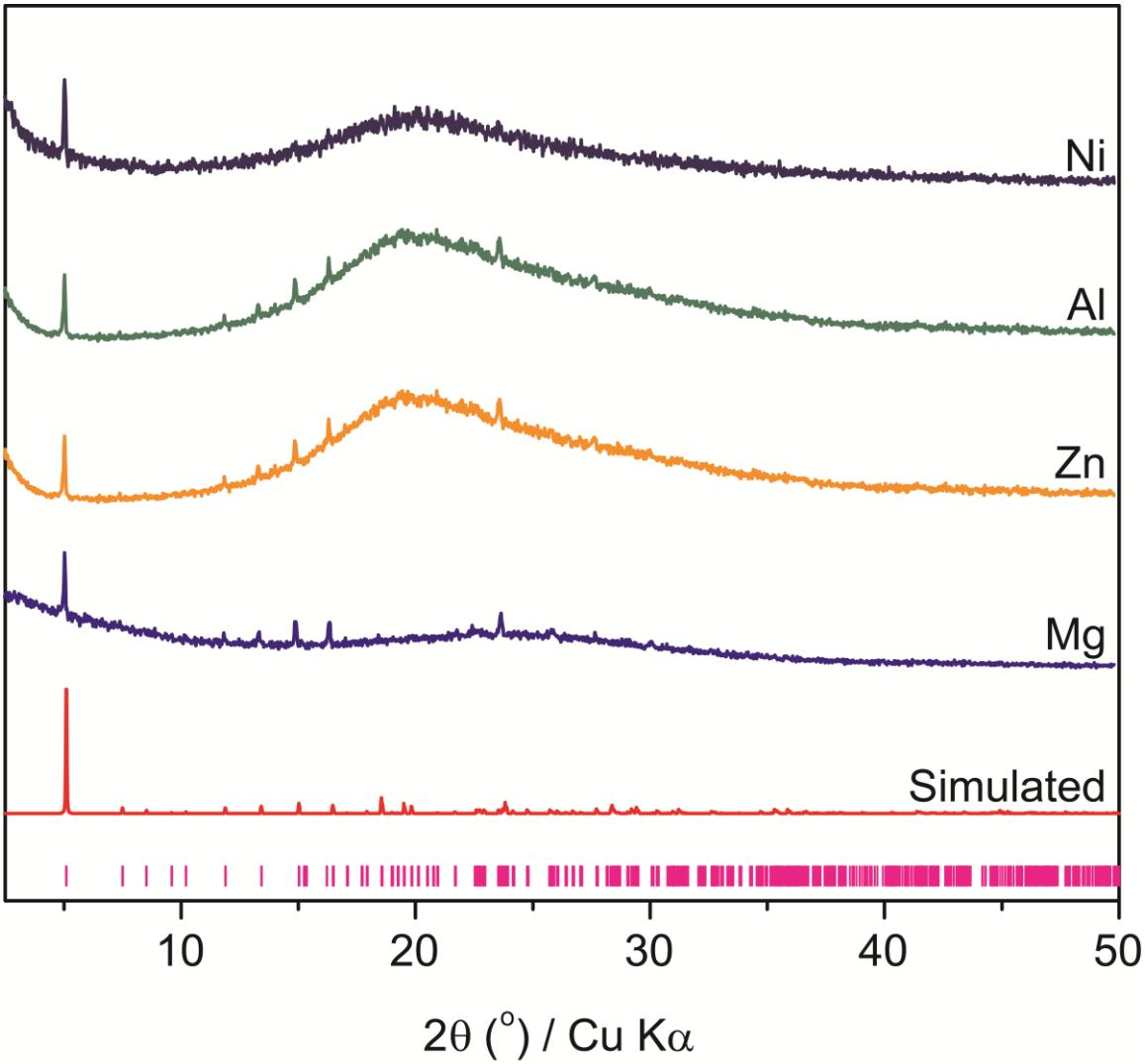

Figure S9. PXRD patterns of the simulated pattern (red) from single crystal MOF-705, and those synthesized with various metal additives.

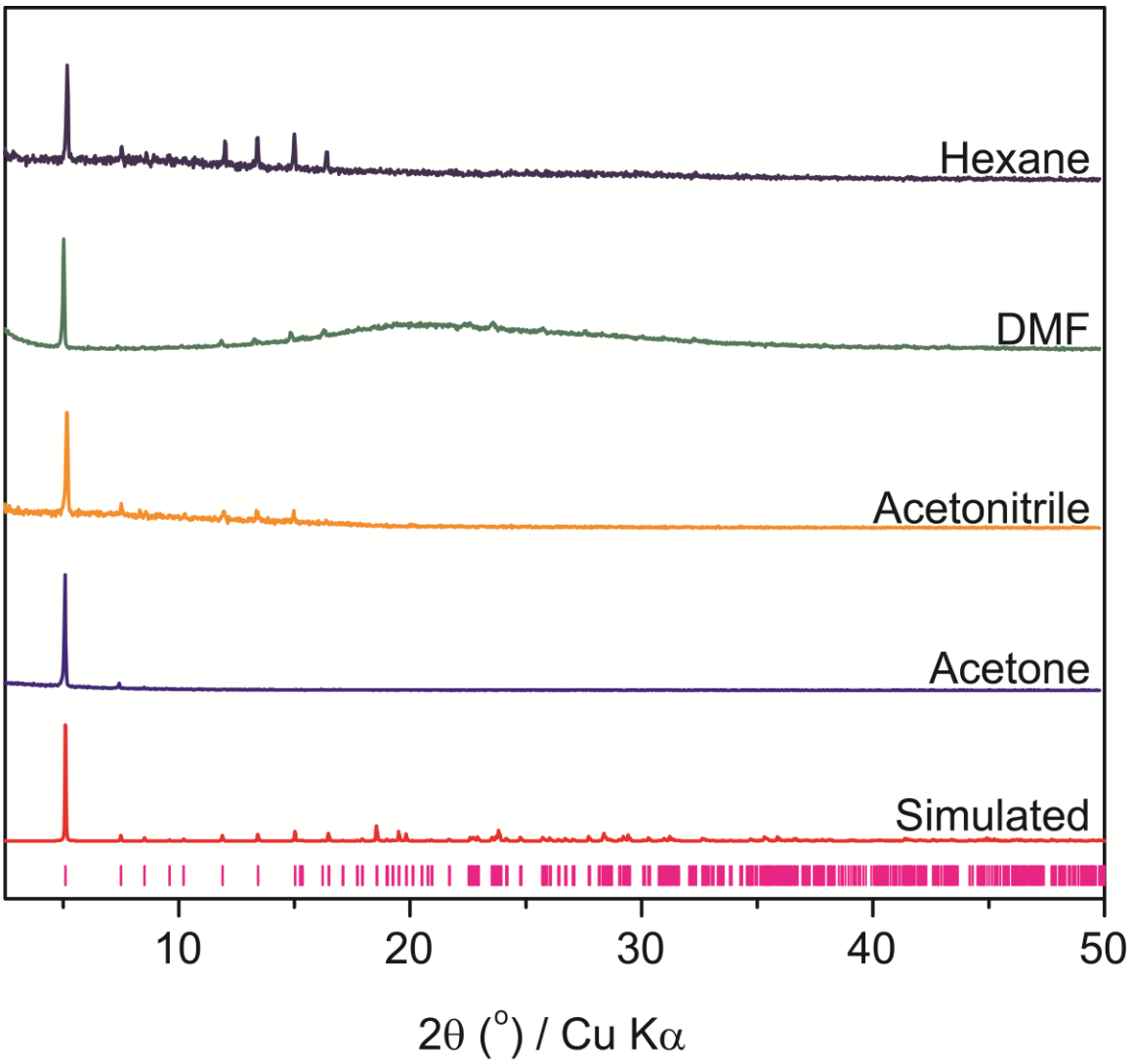

Figure S10. PXRD patterns of simulated pattern from as-synthesized single crystal of MOF-705 and the former immersed in various solvents.

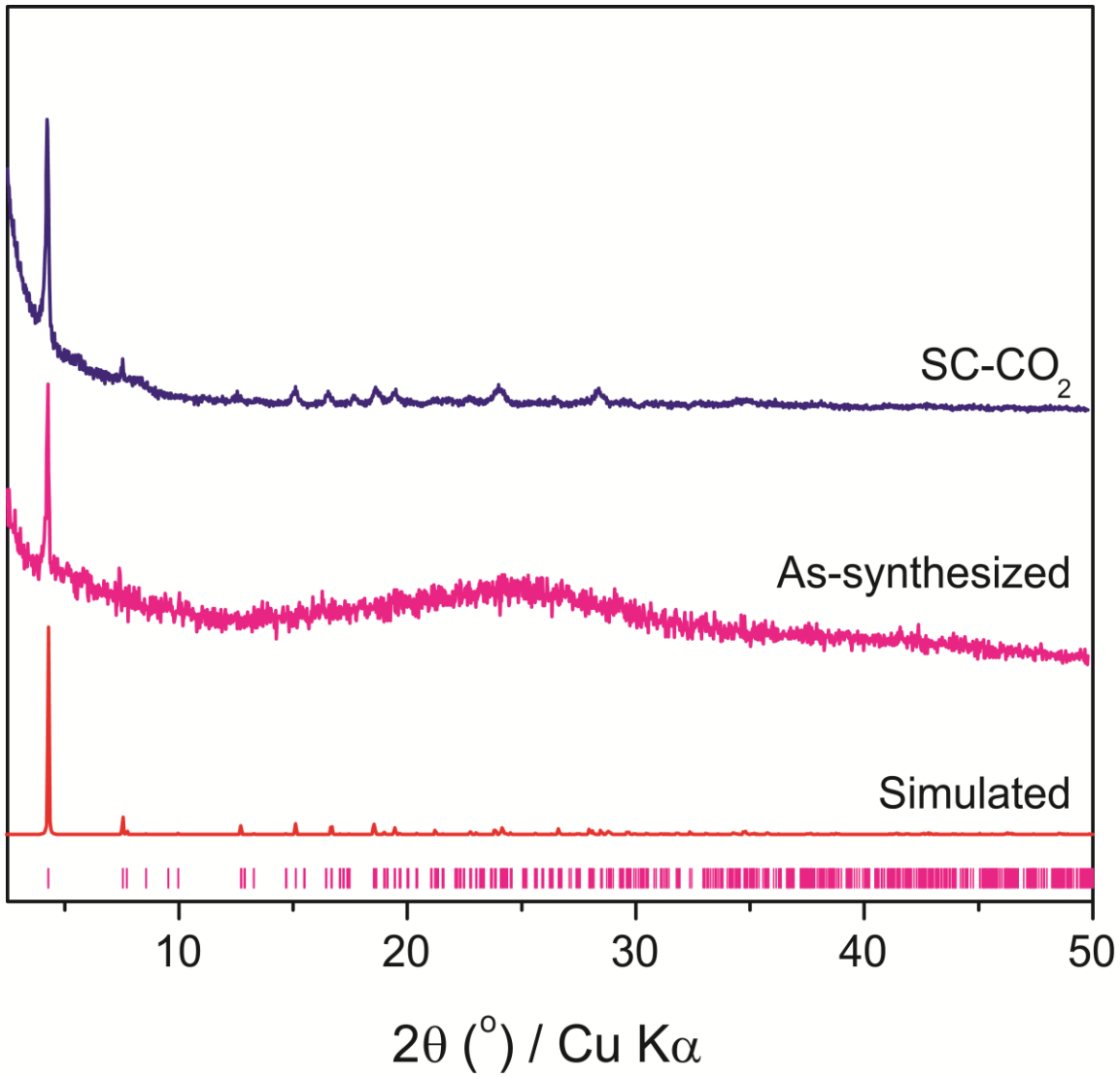

Figure S11. PXRD patterns of simulated from single crystal data (red), as-synthesized (pink) and SC-CO2 activated (purple) of the MOF-706.

4.5 Thermogravimetric Analyses (TGA)

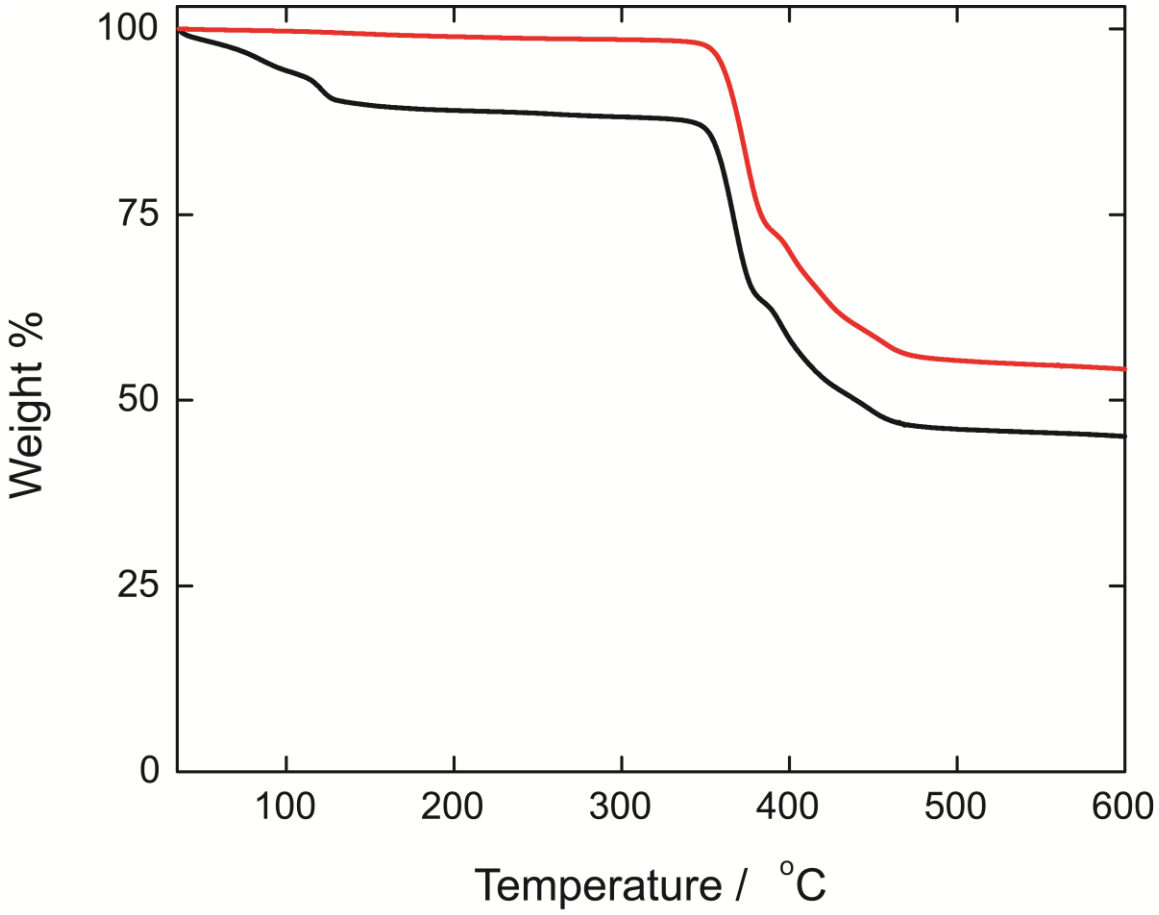

Figure S12. TGA trace for MOF-705 at a heating rate of 5 °C min^{-1} under N_2 flow. The black curve is the activated MOF using SC-CO_2 from methanol, and red is the MOF fully activated using heat under vacuum.

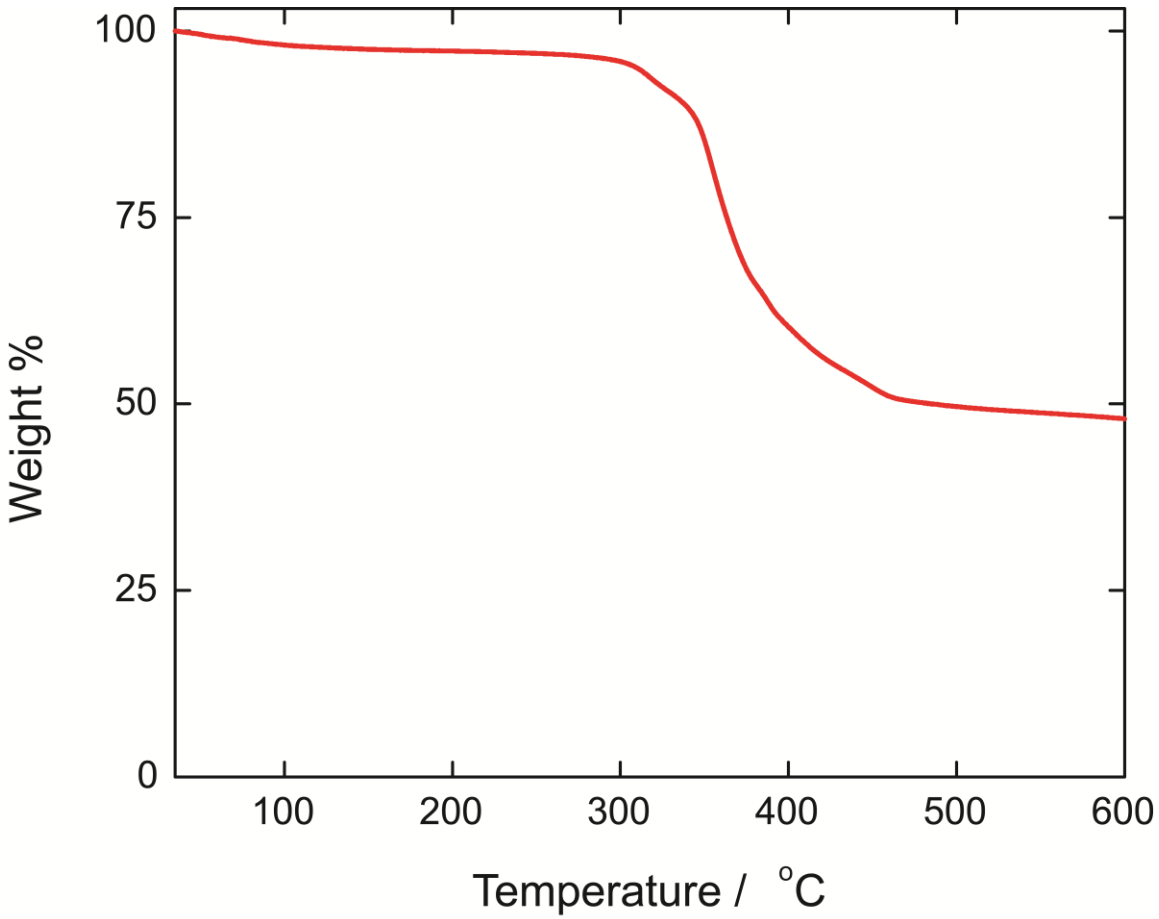

Figure S13: TGA trace for SC-CO_2 activated MOF-706 at a heating rate of 5 °C min^{-1} under N_2 flow.

5. Sorption measurements

5.1 N_2 uptake

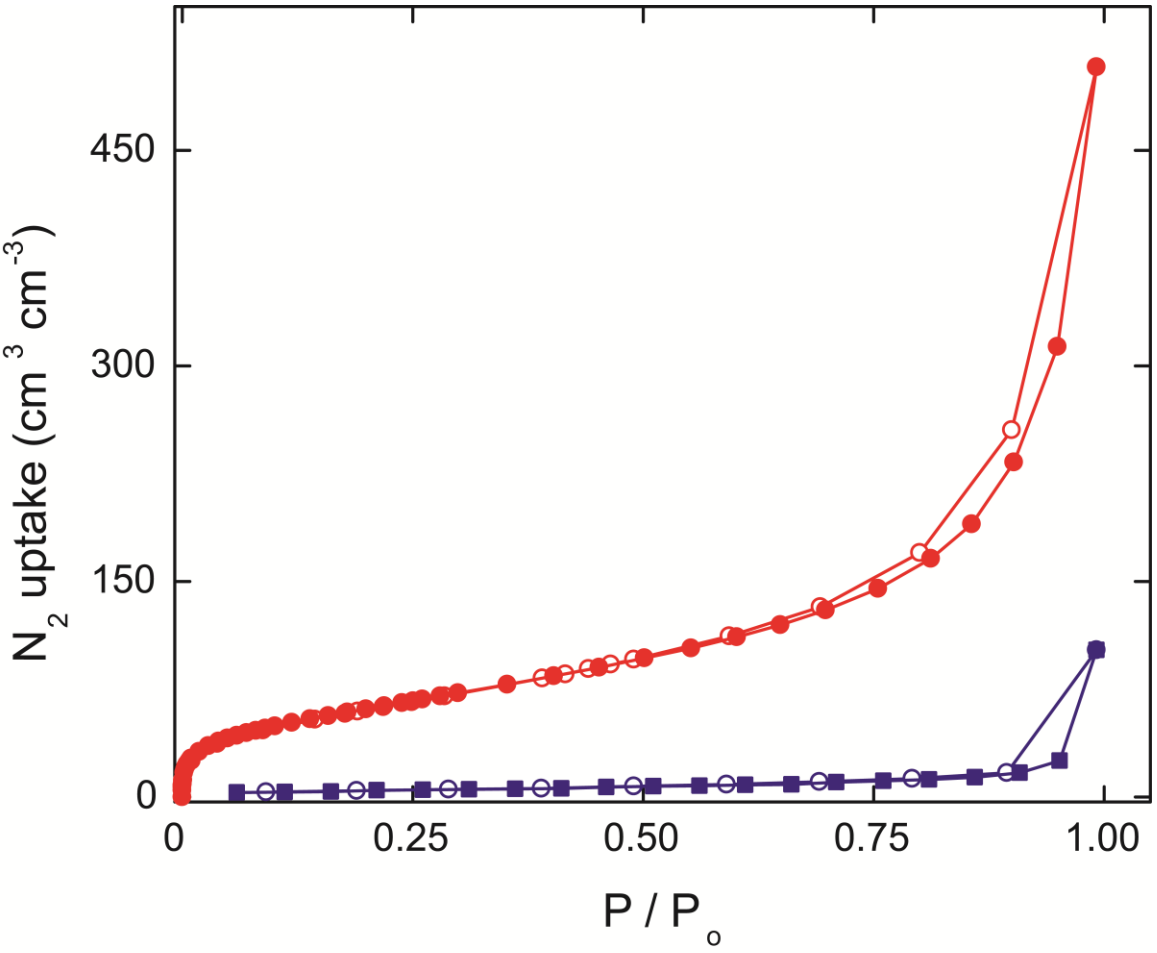

Figure S14. N_2 isotherms for MOF-705 at 77 K. Blue is after SC-CO_2 activationed while red is the heat activated MOF-705. Filled and open symbols represent adsorption and desorption branches, respectively. The connecting curves are guides for the eye.

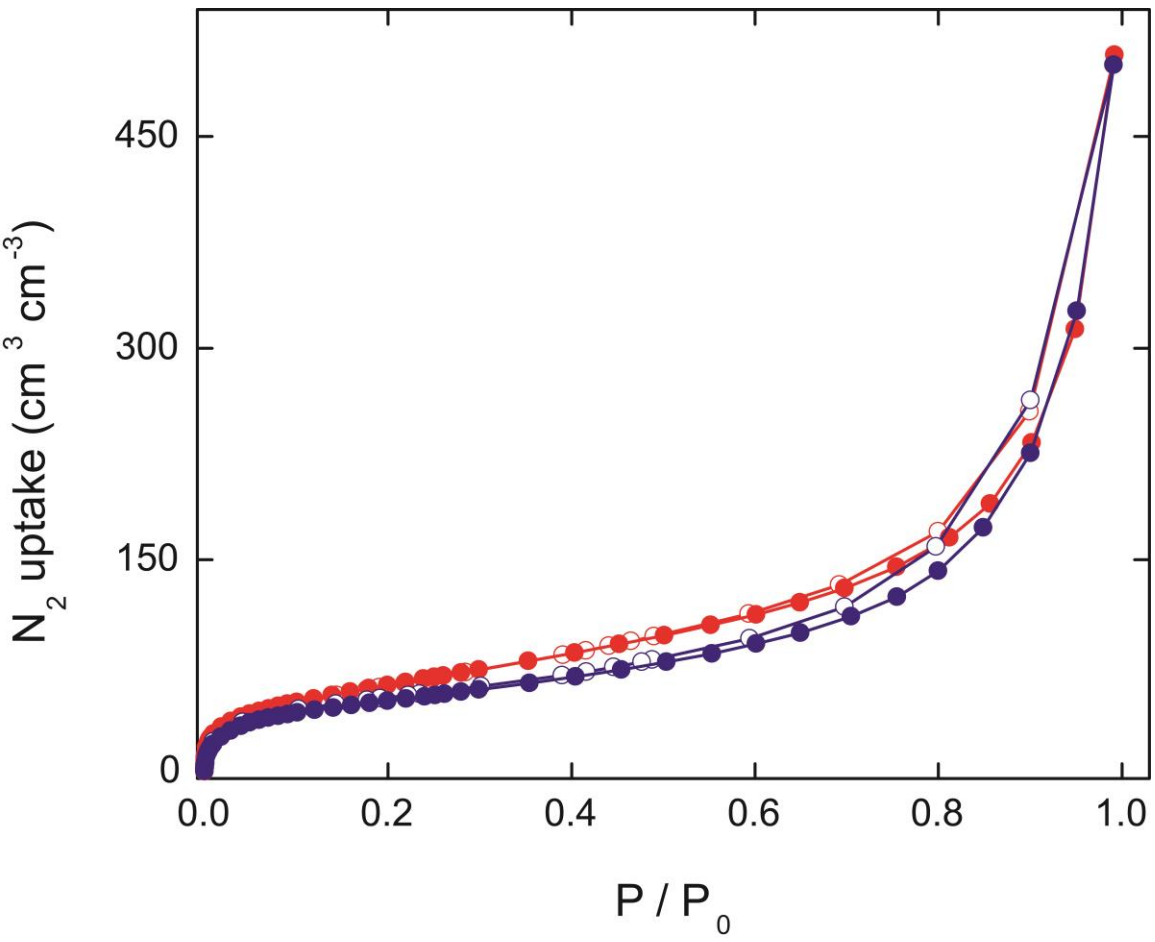

Figure S15. Comparison of N_2 isotherms for fully activated MOF-705 (red) and MOF-706 (blue) at 77 K. Filled and open symbols represent adsorption and desorption branches, respectively. The connecting curves are guides for the eye.

5.2 CO_2 uptake

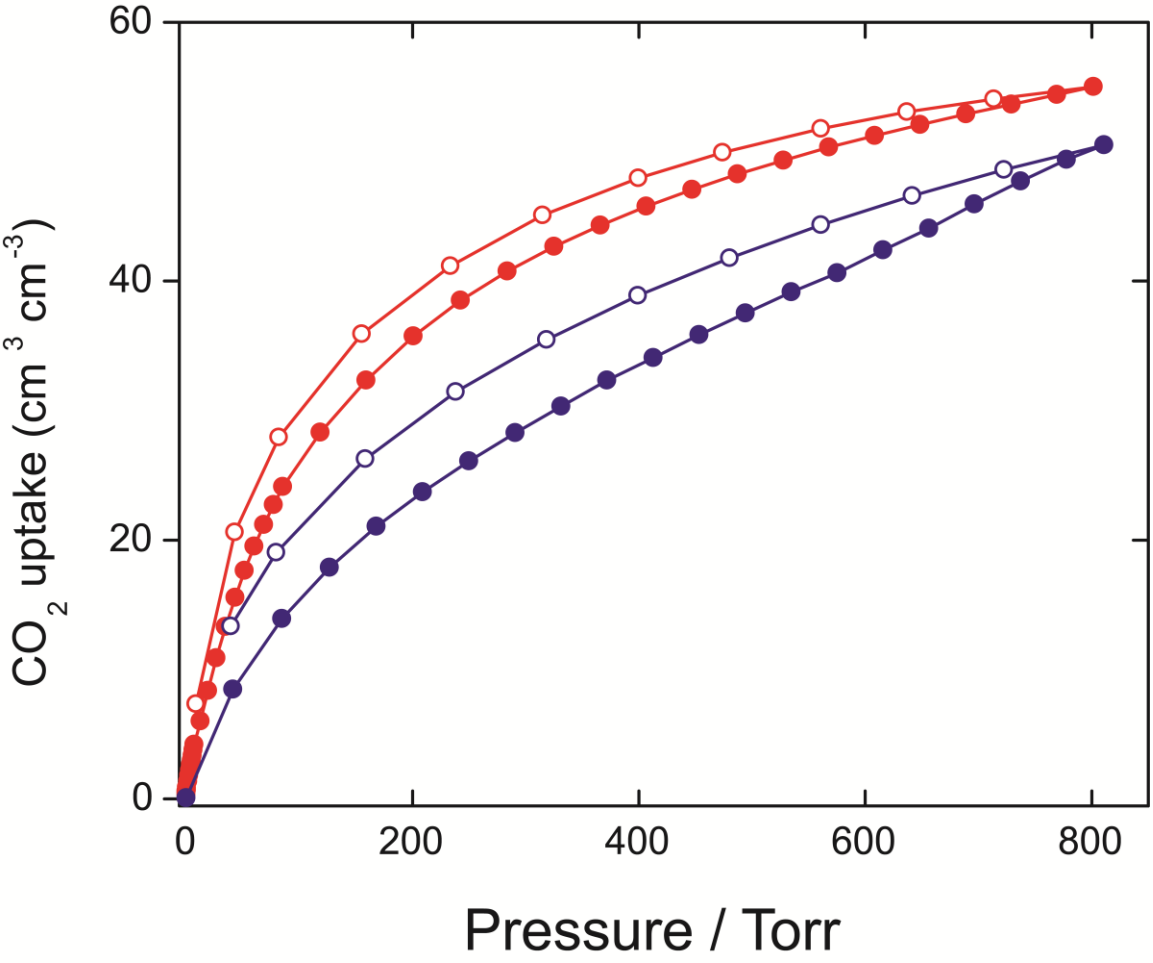

Figure S16. CO_2 isotherms for MOF-705 at 298 K. Blue is MOF-705 treated with SC-CO_2 while red is the heat activated MOF-705. Filled and open symbols represent adsorption and desorption branches, respectively. The connecting curves are guides for the eye.

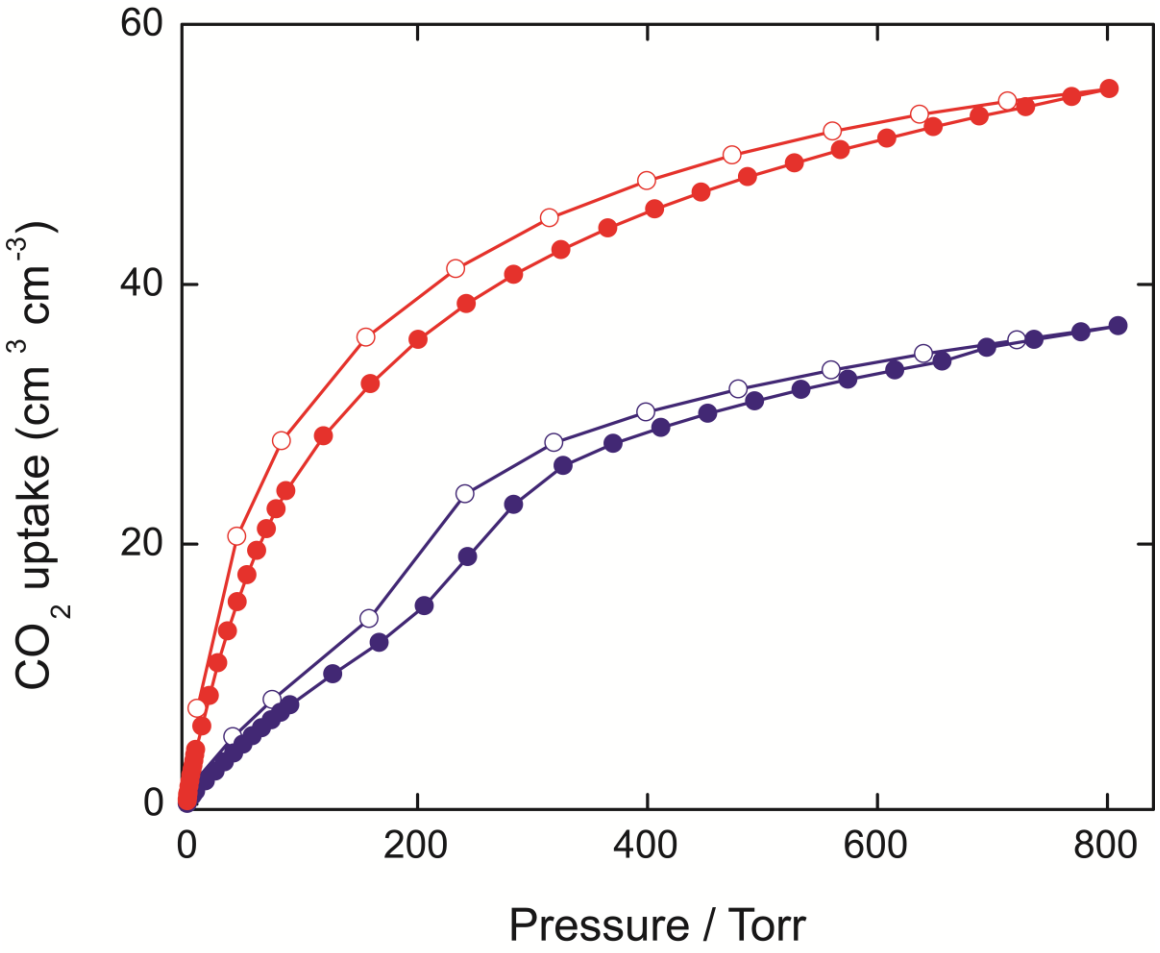

Figure S17. Comparison of CO_2 isotherms for fully activated MOF-705 and MOF-706 at 298 K. Filled and open symbols represent adsorption and desorption branches, respectively. The connecting curves are guides for the eye.

5.3 N_2 and CO_2 sorption at 273 and 298 K

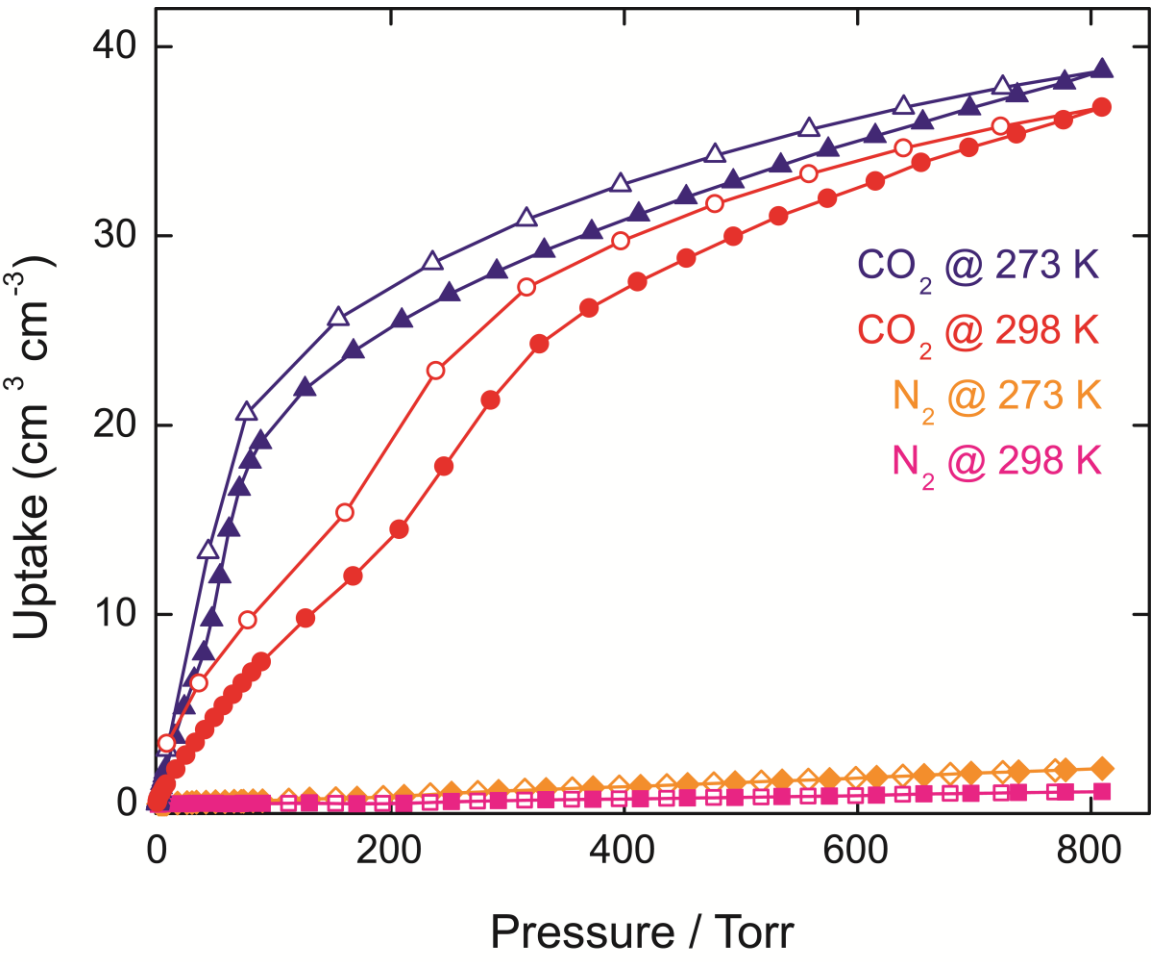

Figure S18. CO_2 and N_2 isotherms for MOF-706 measured at 273 and 298 K. Filled and open symbols represent adsorption and desorption branches, respectively. The connecting curves are guides for the eye.

6. Breakthrough

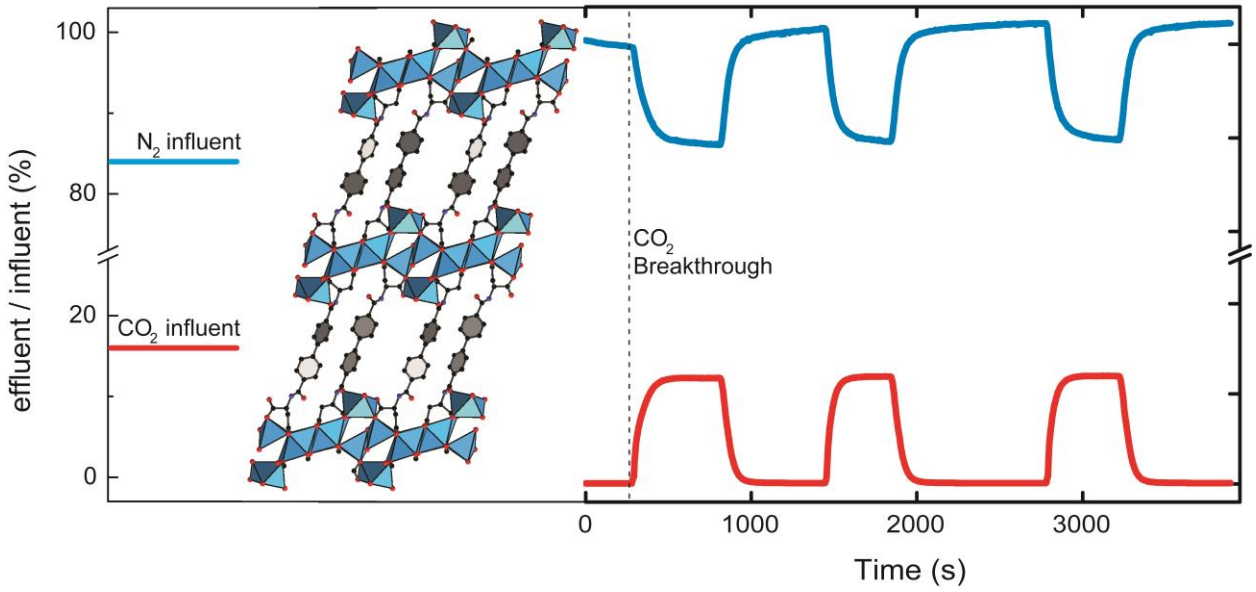

Figure S19. MOF-706 breakthrough cycles under dry conditions.

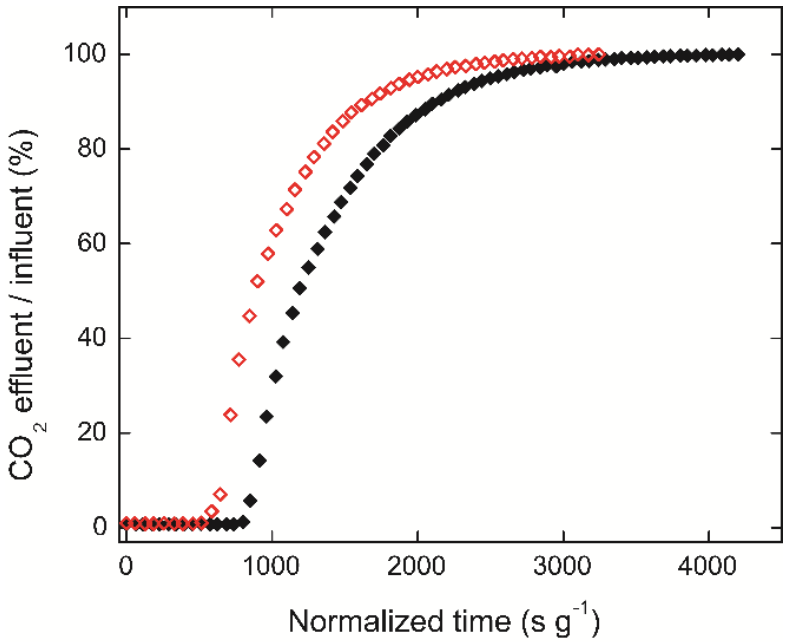

Figure S20. Breakthrough curves for MOF-705 (black filled markers) and MOF-706 (red empty markers).

7. NMR spectra

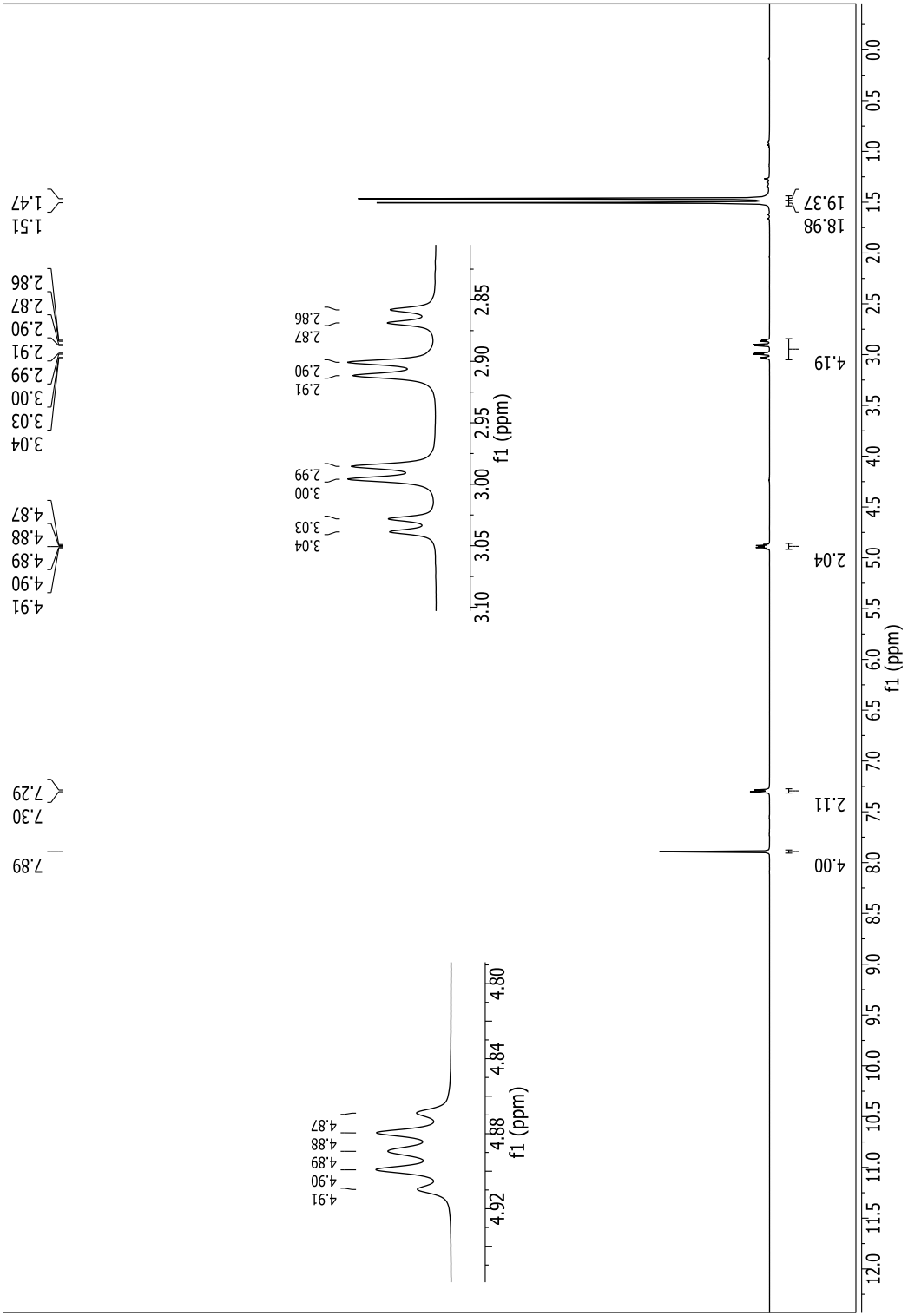

Figure S21. ^{1}H NMR spectra of tetra-*tert*-butyl-2,2'-(terephthaloylbis(azanediyl))(2*S*,2'*S*)-disuccinate (**5**).

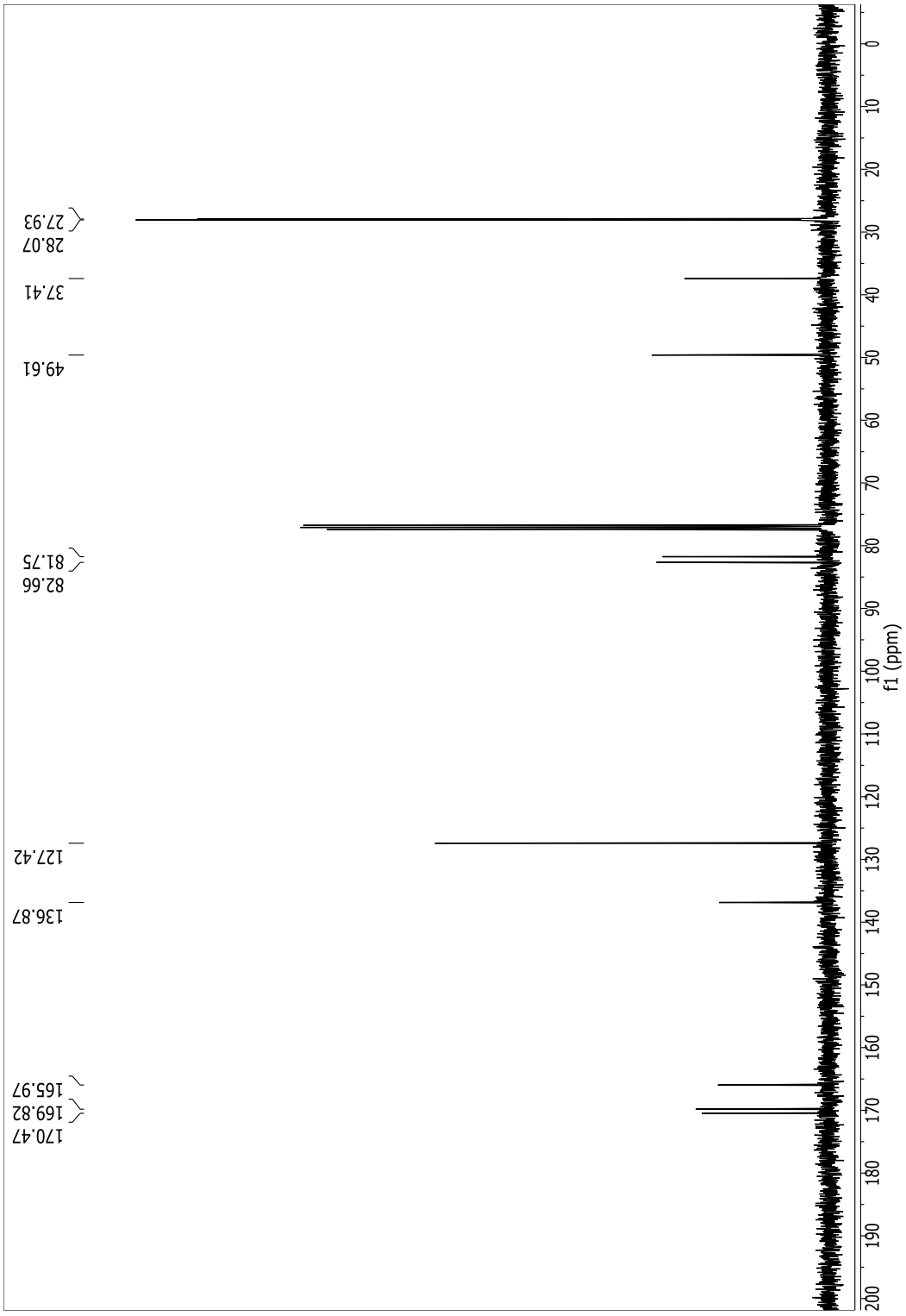

Figure S22. ^{13}C NMR spectrum of tetra-*tert*-butyl-2,2'-(terephthaloylbis(azanediyl))(2*S*,2'*S*)-disuccinate (**5**).

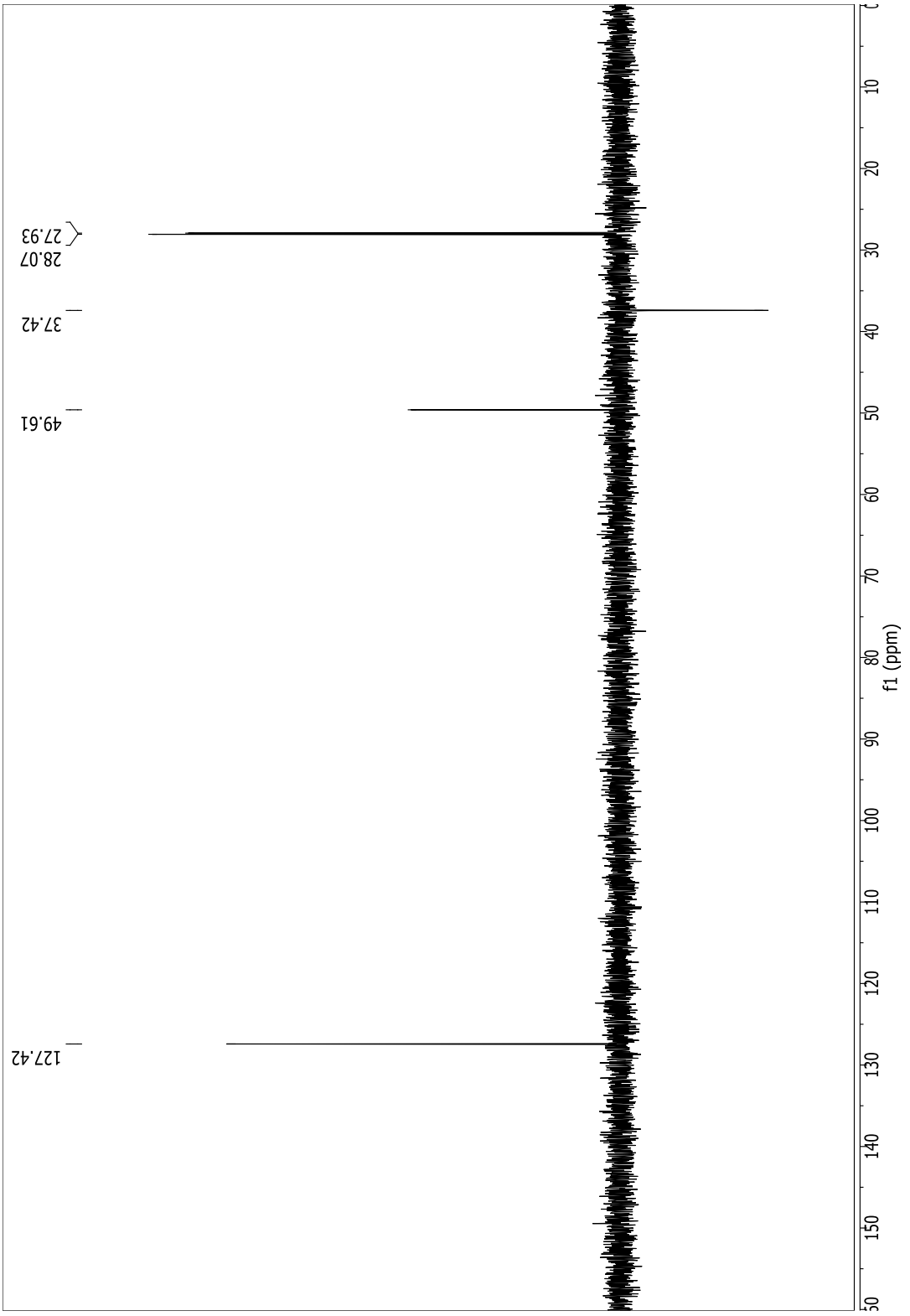

Figure S23. DEPT NMR spectrum of tetra-*tert*-butyl-2,2'-(terephthaloylbis(azanediyl))(2*S*,2'*S*)-disuccinate (**5**).

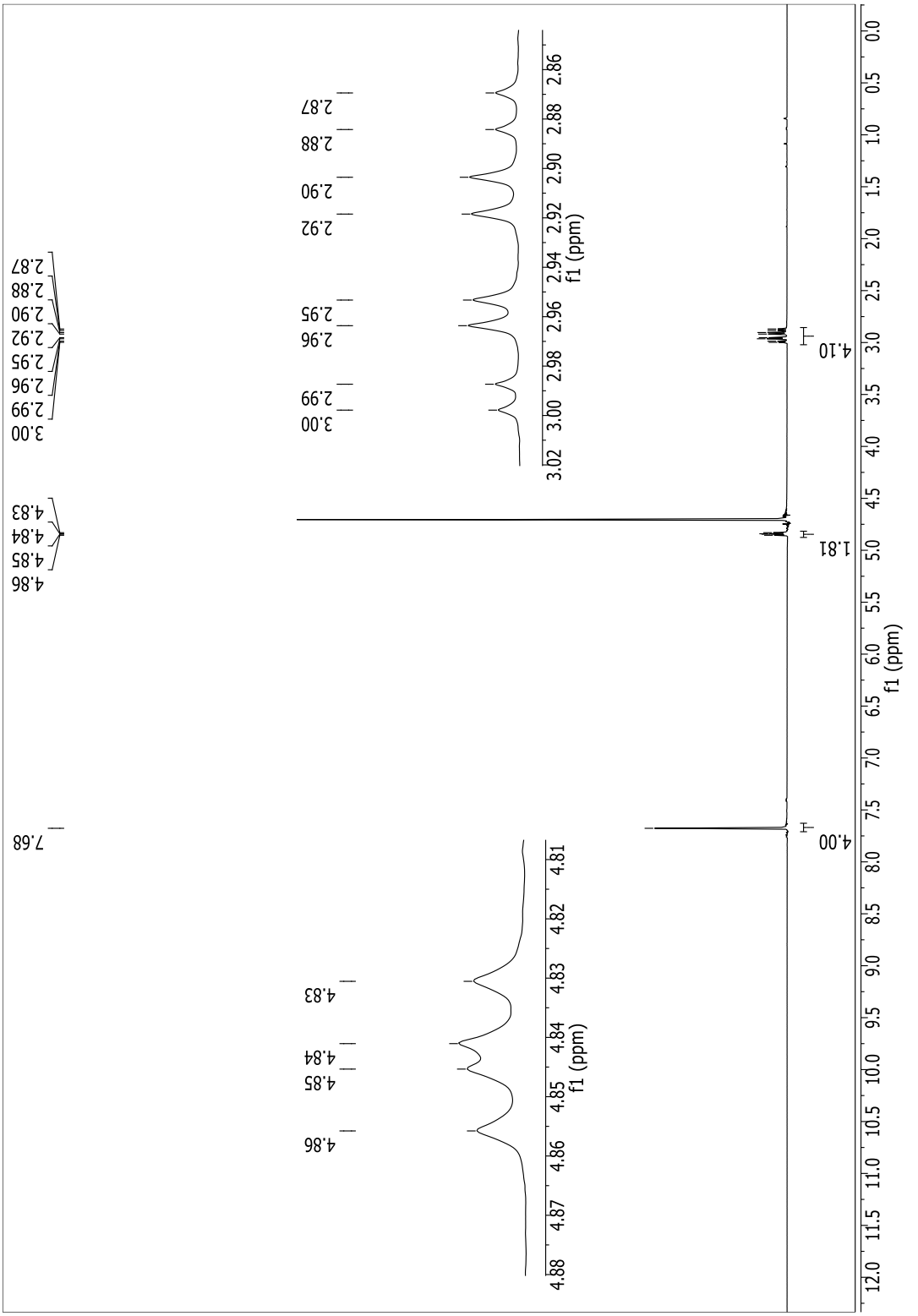

Figure S24. ^{1}H NMR spectrum of (2*S*,2'*S*)-2,2'-(terephthaloylbis(azanediyl))disuccinic acid (**1**).

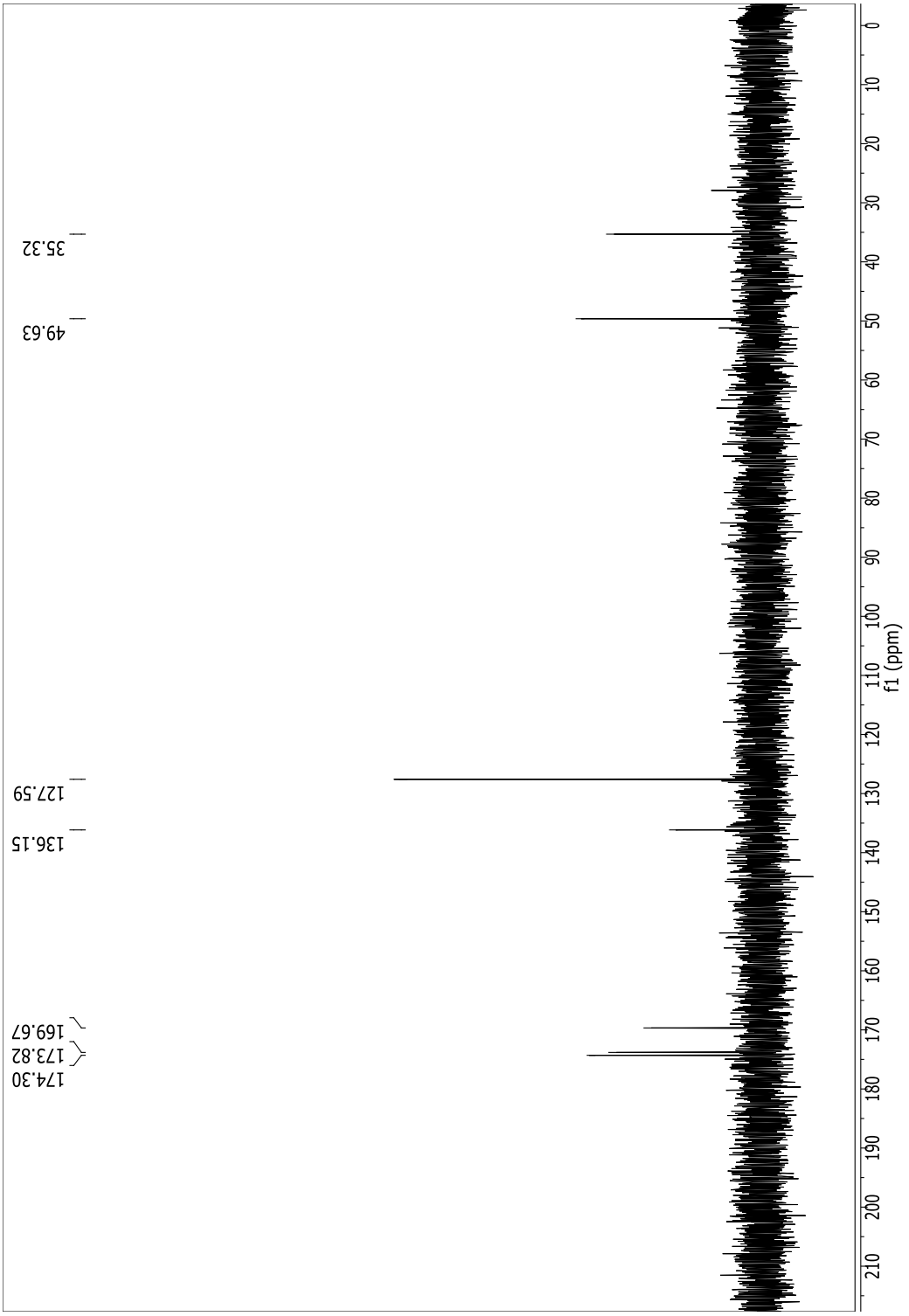

Figure S25. ^{13}C NMR spectrum of (2*S*,2'*S*)-2,2'-(terephthaloylbis(azanediyl))disuccinic acid (**1**).

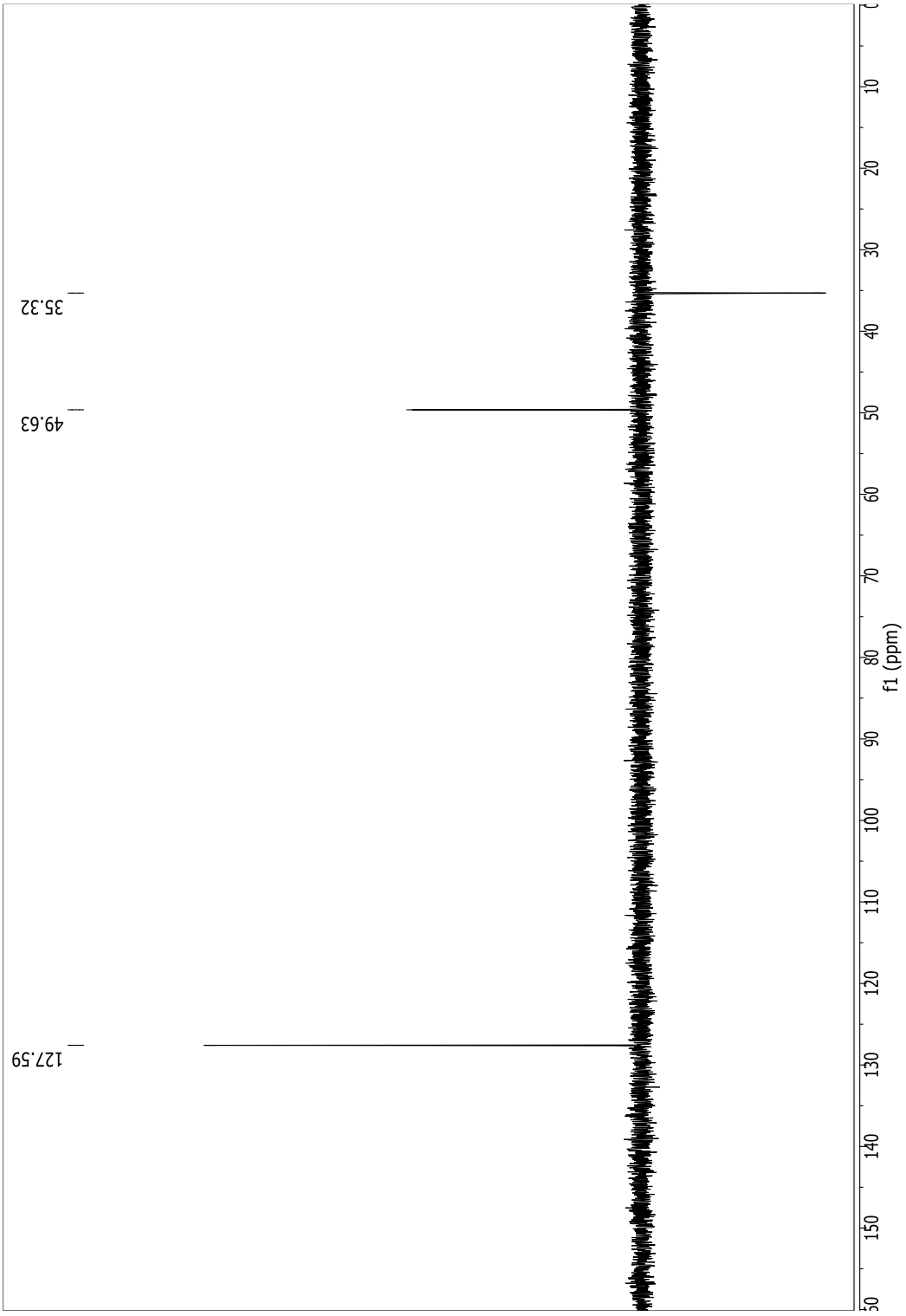

Figure S26. DEPT NMR spectrum of (2*S*,2'*S*)-2,2'-(terephthaloylbis(azanediyl))disuccinic acid (**1**).

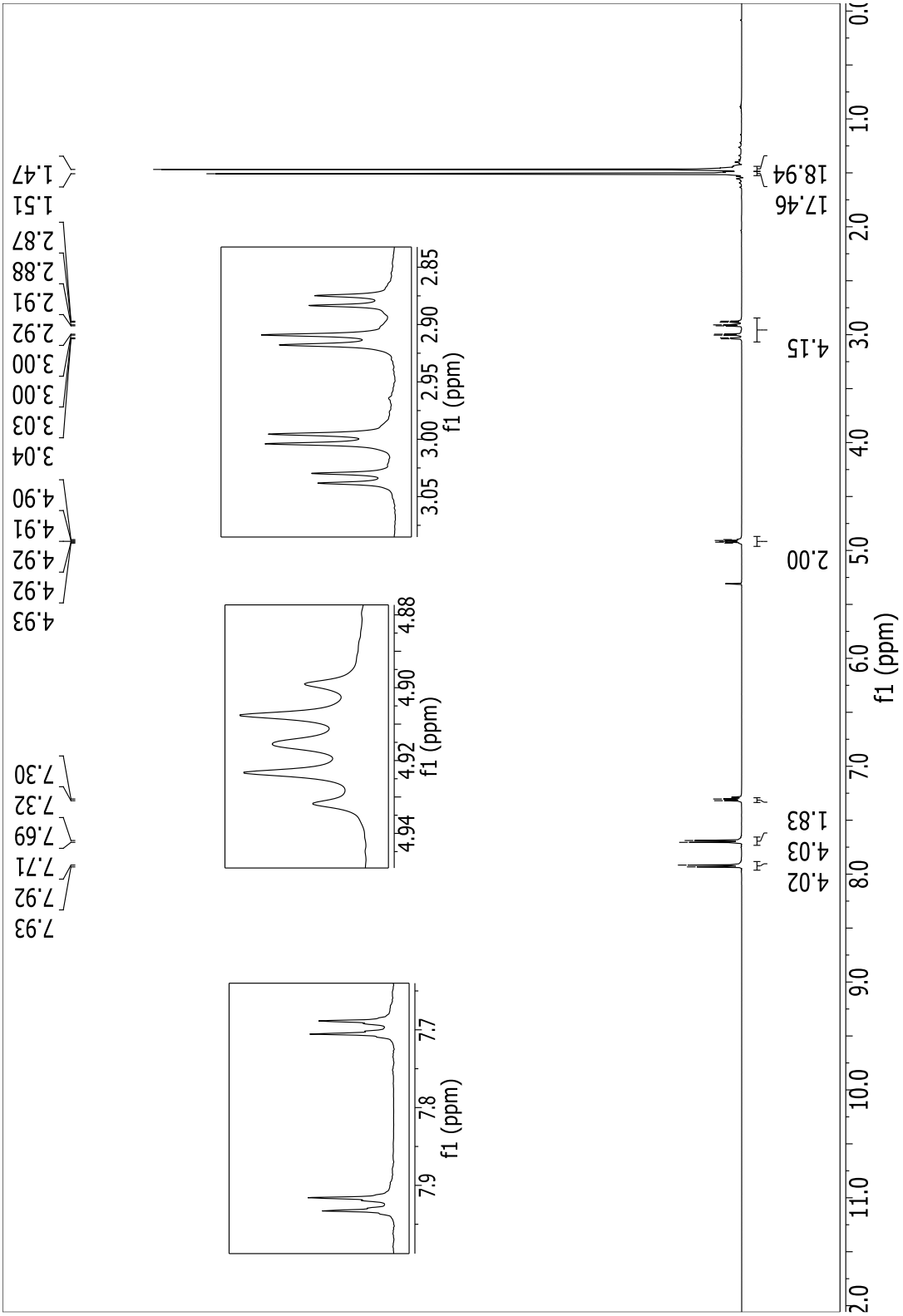

Figure S27. [1]H NMR spectrum of tetra-*tert*-butyl-2,2'- (([1,1'-biphenyl]-4,4'-dicarbonyl) bis(azanediyl))(2*S*,2'*S*)-disuccinate (**7**).

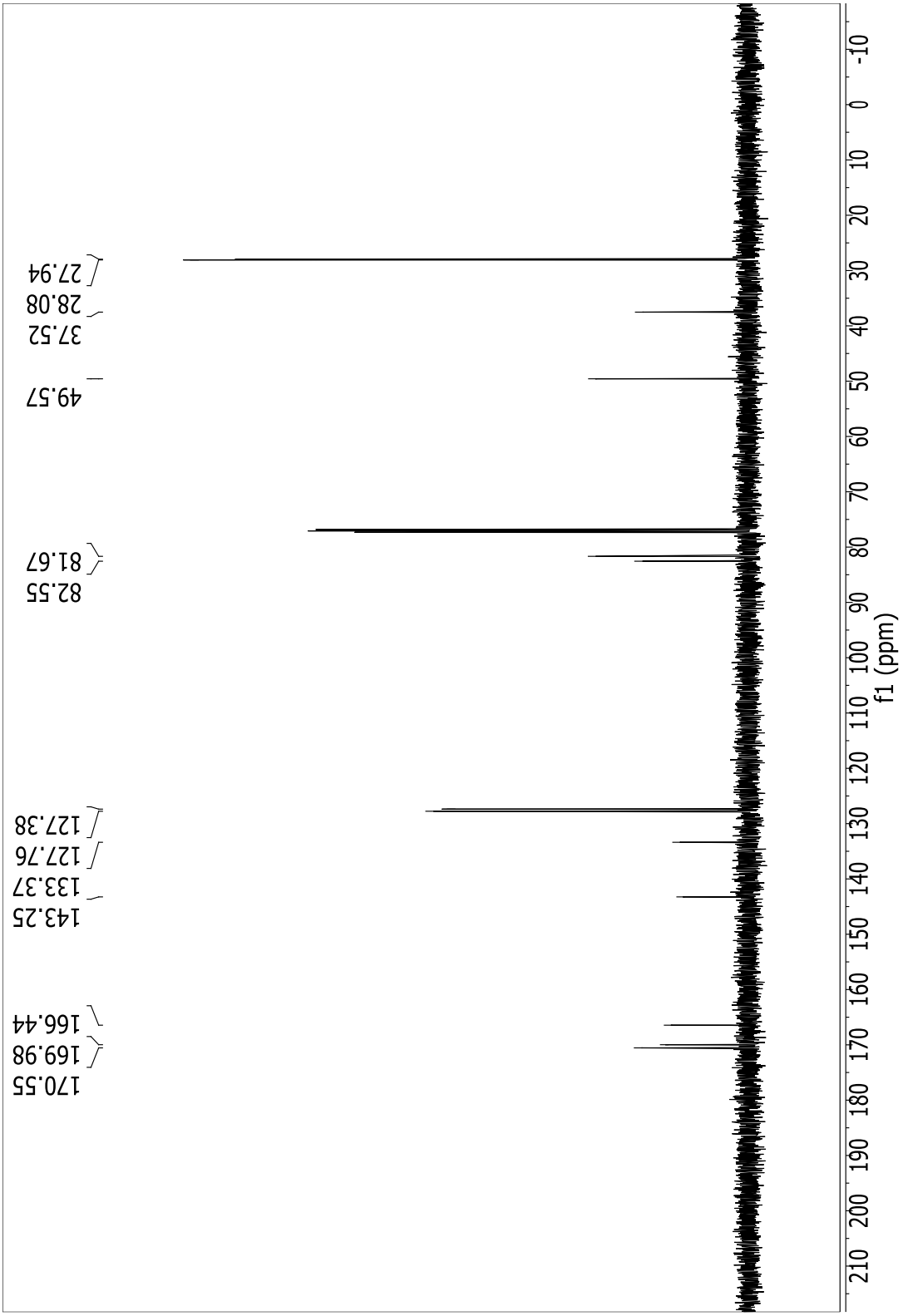

Figure S28. ^{13}C NMR spectrum of tetra-*tert*-butyl-2,2'-(([1,1'-biphenyl]-4,4'-dicarbonyl) bis(azanediyl))(2*S*,2'*S*)-disuccinate (**7**).

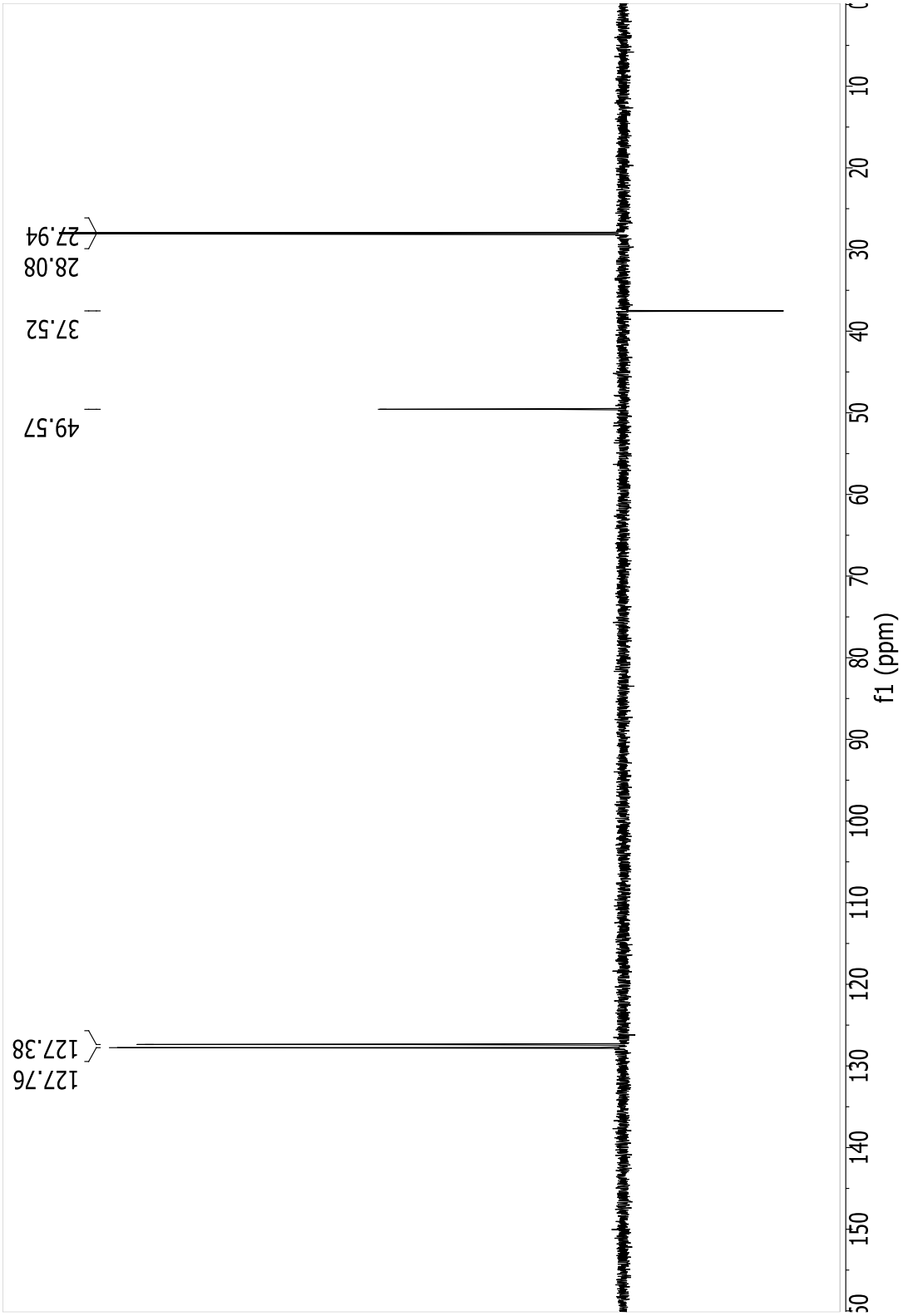

Figure S29. DEPT NMR spectrum of tetra-*tert*-butyl-2,2'-(([1,1'-biphenyl]-4,4'-dicarbonyl) bis(azanediyl))(2*S*,2'*S*)-disuccinate (**7**).

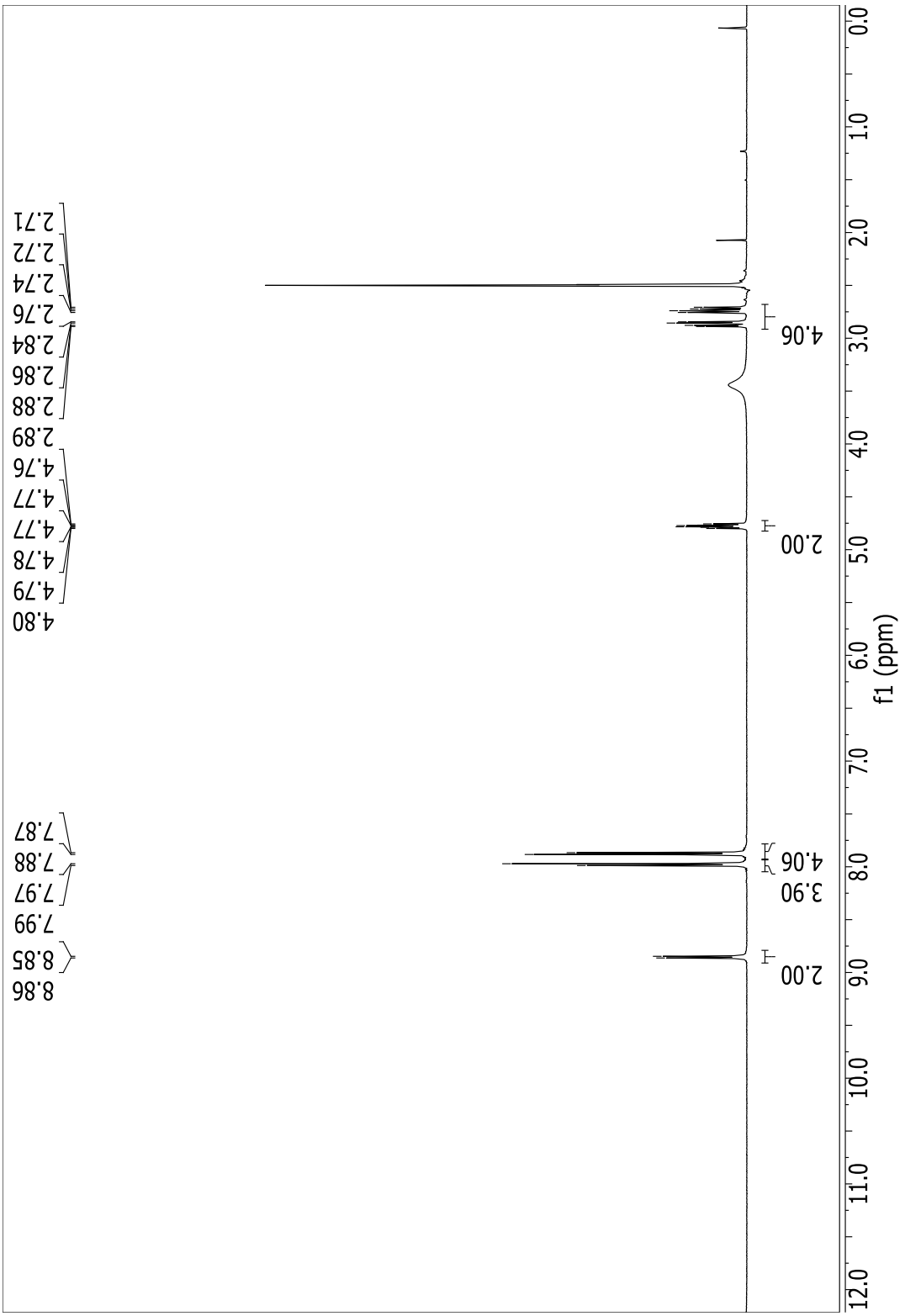

Figure S30. ^{1}H NMR spectrum of (2*S*,2'*S*)-2,2'-(([1,1'-biphenyl]-4,4'-dicarbonyl) bis(azanediyl)) disuccinic acid (**2**).

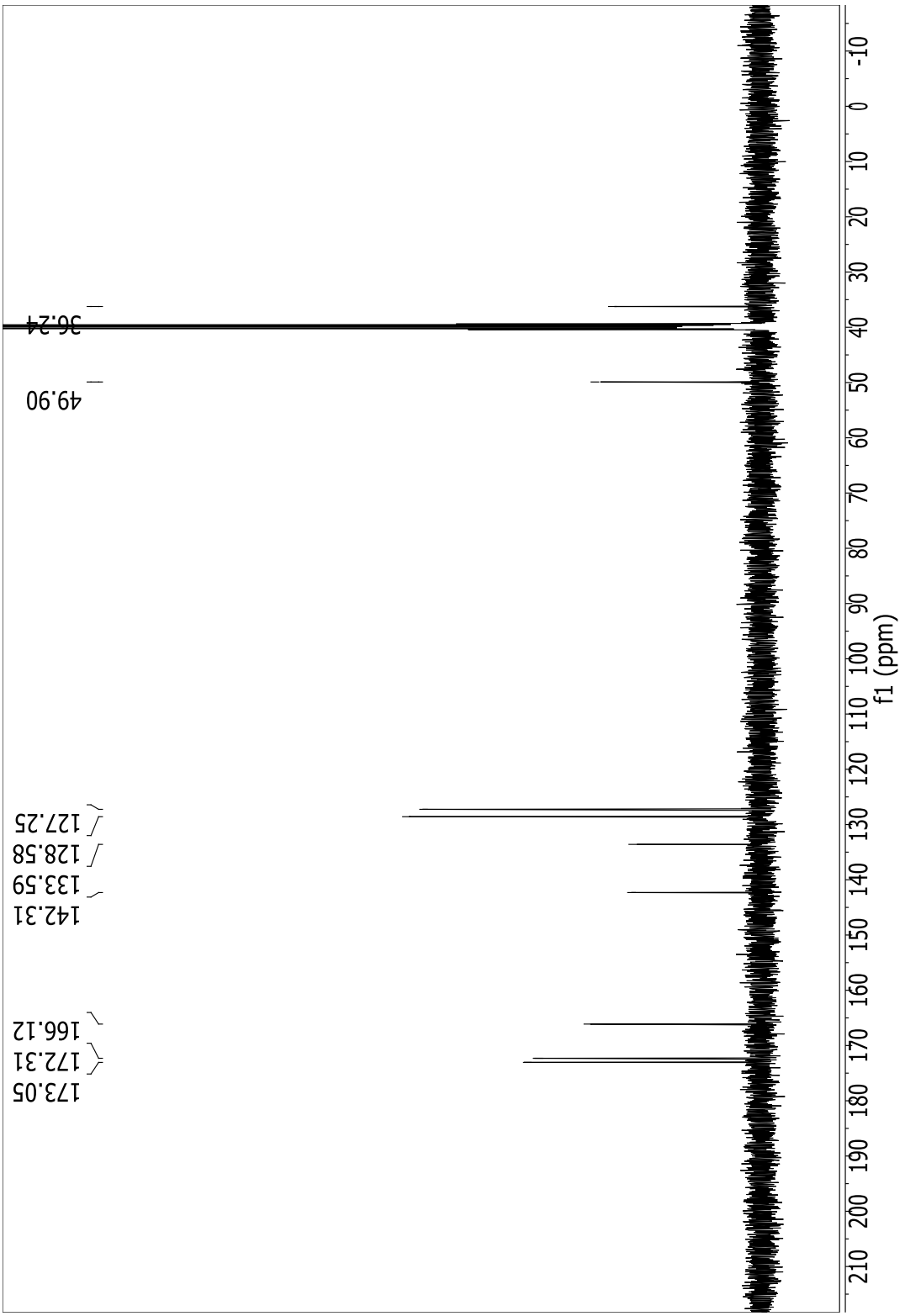

Figure S31. ^{13}C NMR spectrum of (2*S*,2'*S*)-2,2'-(([1,1'-biphenyl]-4,4'-dicarbonyl) bis(azanediyl)) disuccinic acid (**2**).

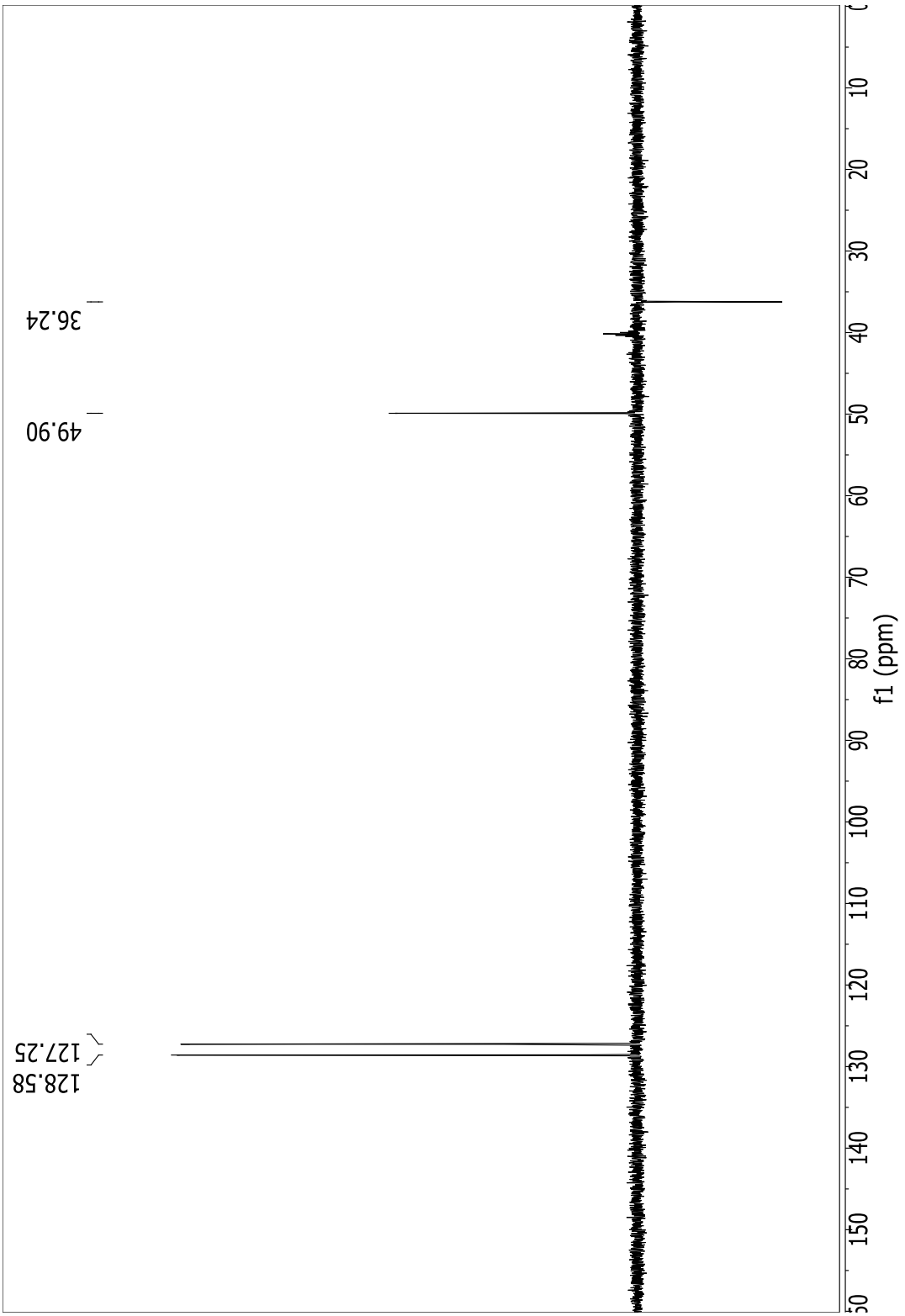

Figure S32. DEPT NMR spectrum of (2*S*,2'*S*)-2,2'-(([1,1'-biphenyl]-4,4'-dicarbonyl)bis(azanediyl))disuccinic acid (**2**).

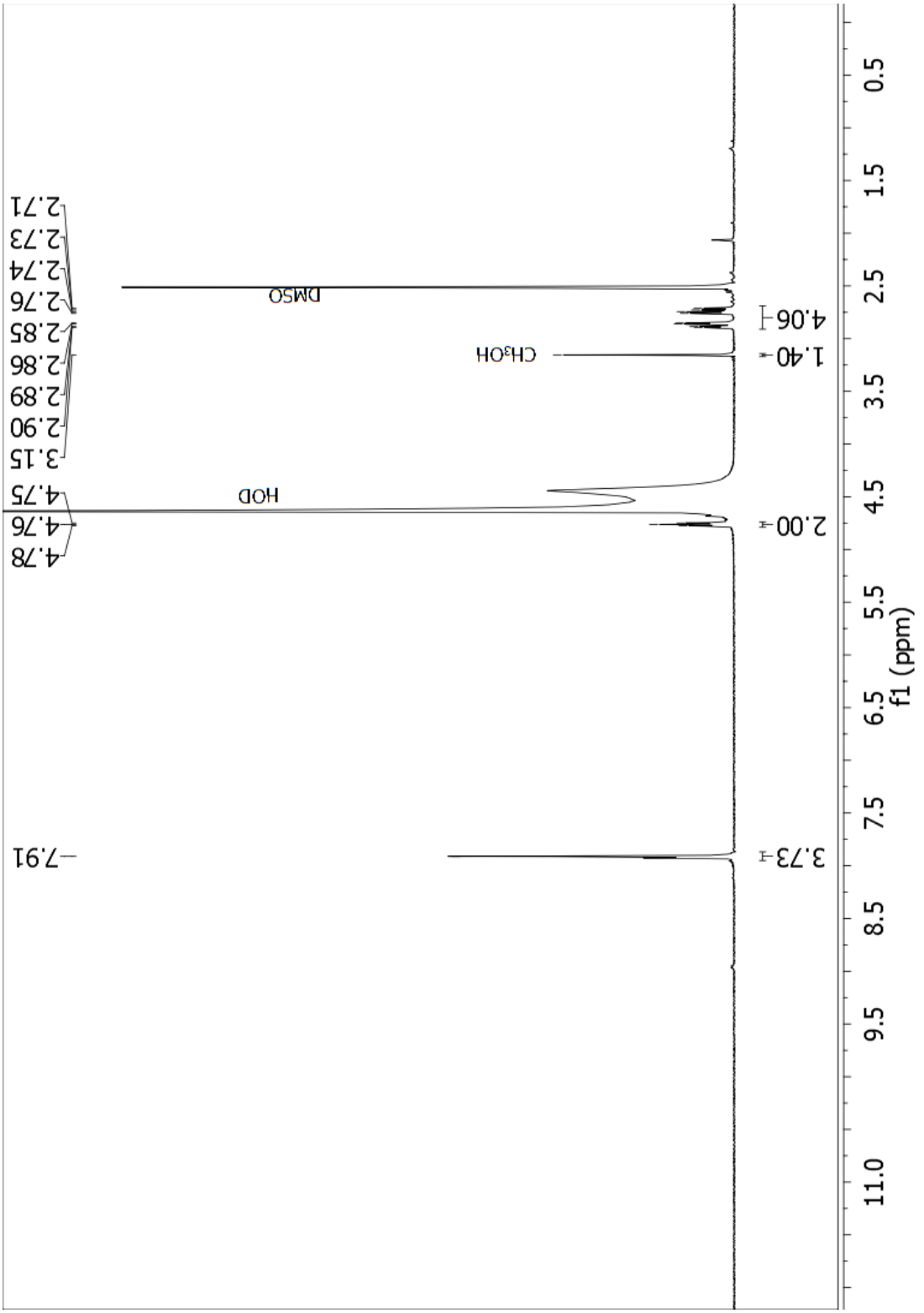

Figure S33. ^{1}H NMR spectrum of digested MOF-705.

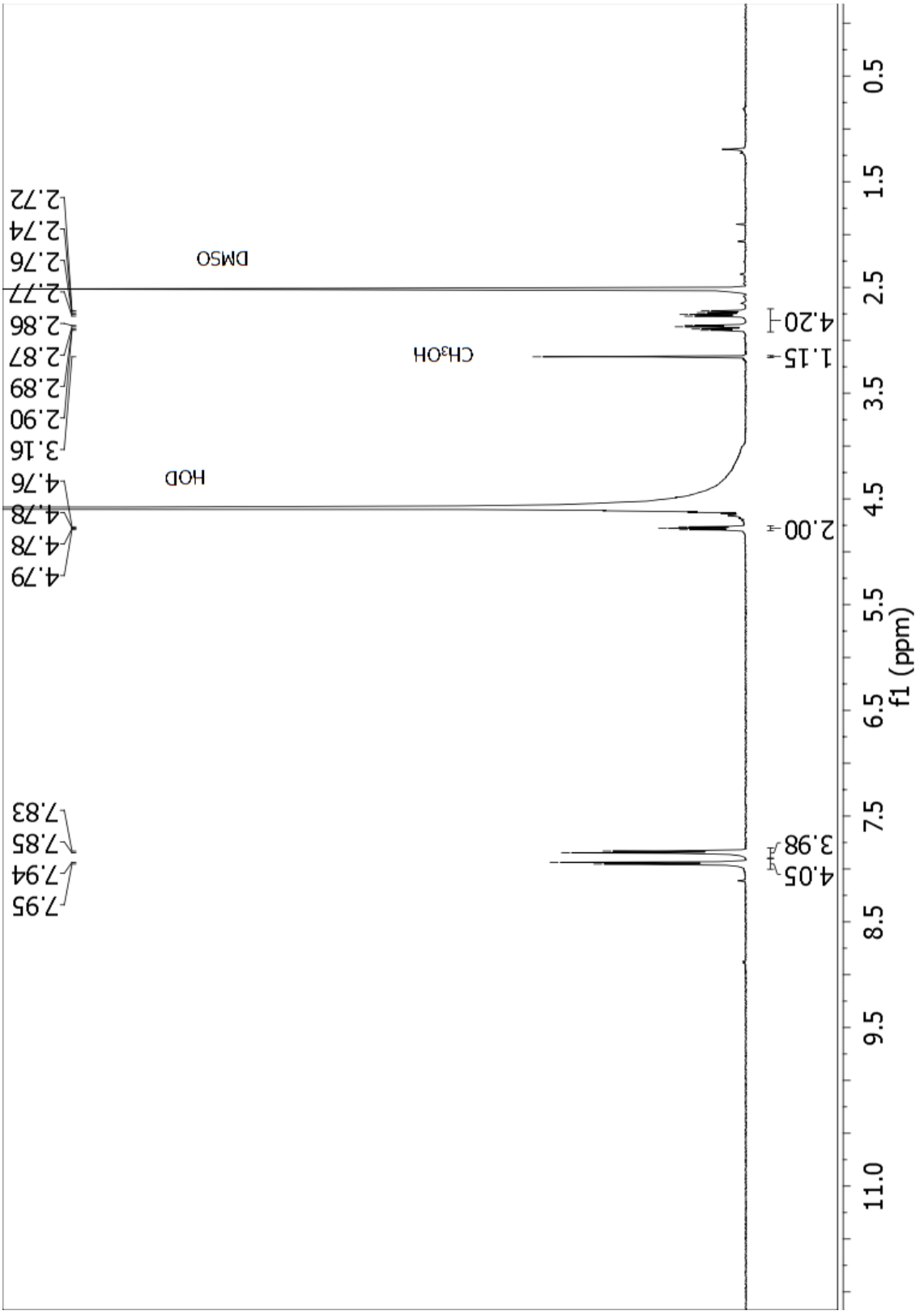

Figure S34. ^{1}H NMR spectrum of digested MOF-706.

8. HPLC

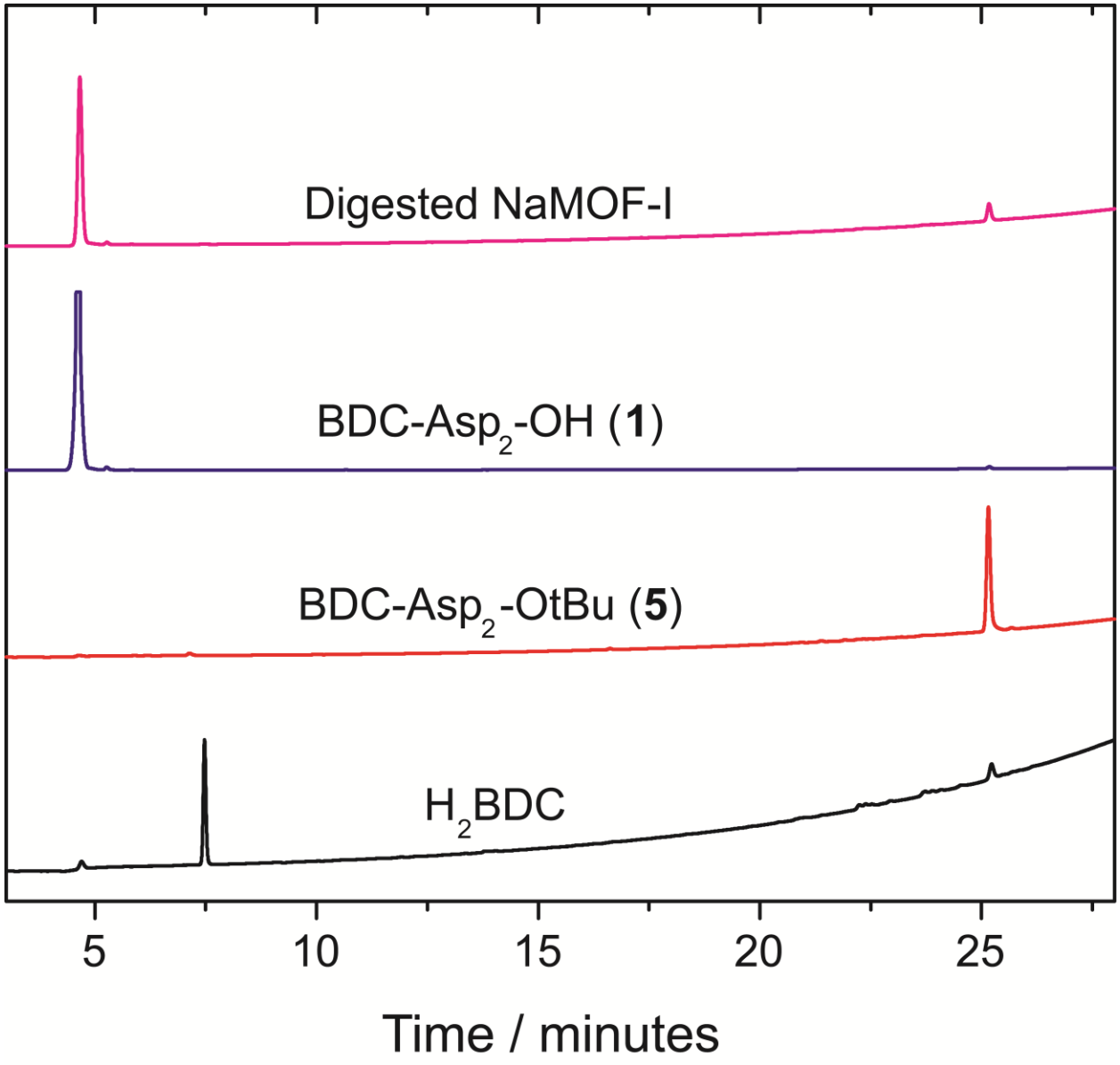

Figure S35. HPLC trace of (bottom to top): terephthalic acid, *tert*-butyl protected intermediate (5**3**), the linker (**1,** H_2BDA), and digested MOF-705.

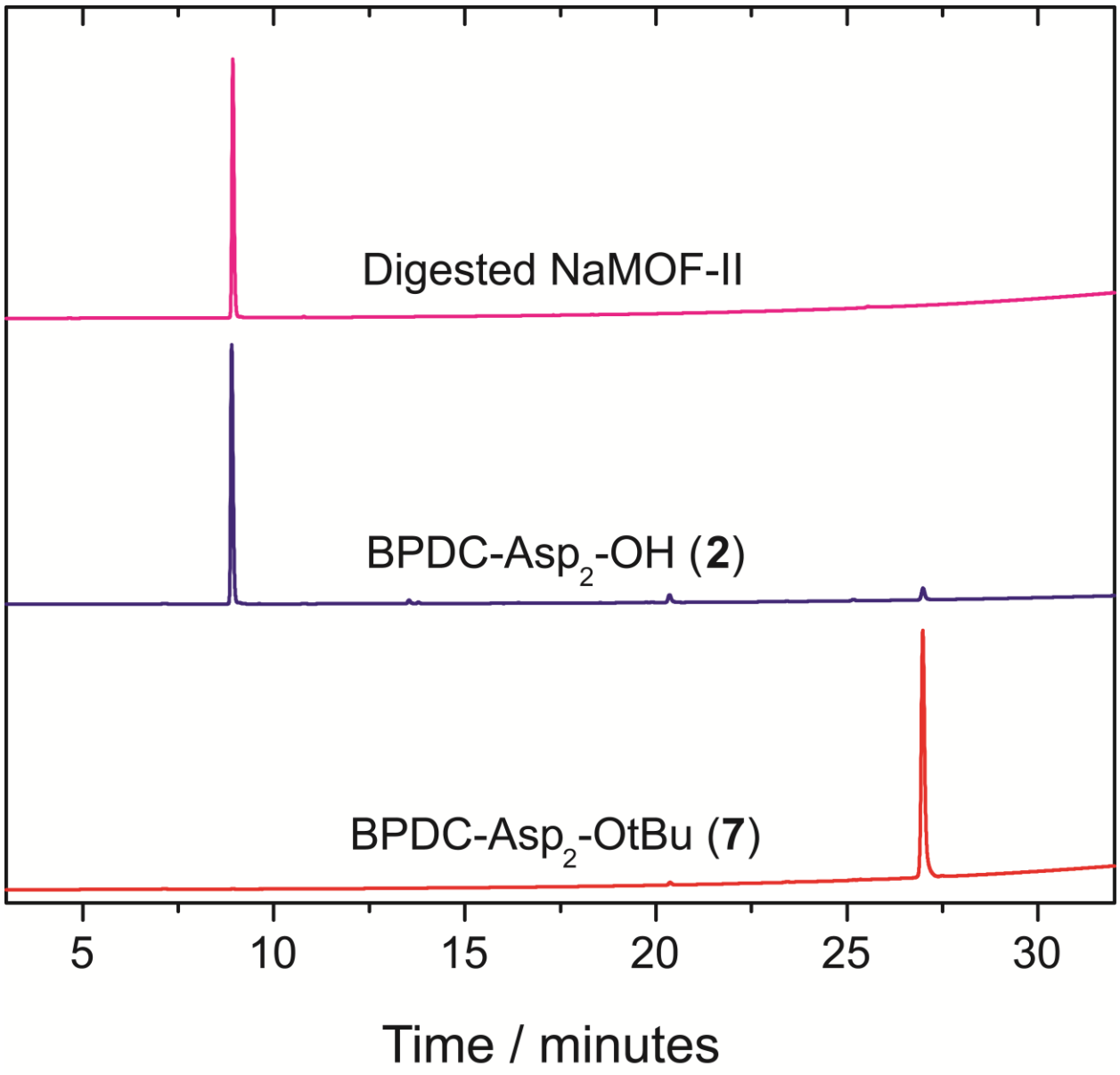

Figure S36. HPLC trace of (bottom to top): *tert*-butyl protected intermediate (**7**), the extended linker (**2,** H_2BPDA), and digested MOF-706. The starting material, H_2BPDC (**6**), was not included because it is insoluble in HPLC solvents suitable for HPLC.

References

1. The addition of $Mg(NO_3)_2 \cdot 6H_2O$ or other metal nitrates such as nickel, zinc and aluminum are crucial for the MOF syntheses. We are not sure regarding their role in the synthesis, however we confirmed that the MOFs do not contain these metal ions by TGA, SXRD, SEM and PXRD. The best crystals were obtained with $Mg(NO_3)_2$ so this was used for scaling up.
2. The reaction can be performed in autoclave as well. It is crucial that the reaction vessel is tightly sealed, otherwise the solvent will evaporate and amorphous phase will form.